PROPOSED ONE MILLION KILOMETER LASER GRAVITATIONAL WAVE ANTENNA IN SPACE

P.L. Bender, J.E. Faller, J.L. Hall, D. Hils, M.A. Vincent
Joint Institute for Laboratory Astrophysics
National Bureau of Standards and University of Colorado
Boulder, Colorado 80309, USA

Telephone (303) 492 6952
Telex 910 940 3441

ABSTRACT

We are investigating the possible use of laser heterodyne measurements between free test masses in three separate spacecraft to observe gravitational waves with periods of roughly 0.1 to 10^6 seconds. The geometry is the same as for a Michelson interferometer with nearly equal arms. The beam splitter is mounted in the test mass in the central spacecraft. A laser in each end spacecraft is phase-locked to the received light, and the output power is sent back to the central spacecraft. The returned beams from the two arms are beat against the laser in the central spacecraft, and the phases of the two resulting Doppler signals are reccorded as a function of time. With 1 mW of visible light from a helium-neon laser and 50 cm diameter transmit-receive optics, the shot noise limit on measuring the fractional difference in length of the two arms is about $10^{-19}/\sqrt{\text{Hz}}$, independent of the arm length. The use of other types of lasers with better efficiency and higher power output may be possible, provided sufficient stability and reliability can be achieved.

One case we have considered involves 10^6 km spacecraft separation, with all three spacecraft located roughly 15° behind the earth in nearly circular orbits about the sun. By choosing the starting conditions correctly, the lengths of the two arms will stay equal to about 1 part in 10^3 over several years. A major goal of the spacecraft design would be to keep the spurious accelerations of the test masses small enough so that the gravitational wave measurements are mainly shot noise limited for periods up to at least 10^4 sec. Unmodeled planetary perturbations will be extremely small out to periods longer than 10^5 sec, so observations on one arm can be used to determine fluctuations in the laser wavelength. The corrected laser wavelength then is used to measure the difference in length of the two arms. With this approach, the stability of helium-neon lasers carefully locked to Fabry-Perot cavities appears to be adequate.

For periodic sources and a 10^6 sec measurement time, the strain sensitivity would be about 10^{-22} over the period range from 10 to 10^4 sec. This range includes the following expected observable sources : a few known rotating binaries ; perhaps 100 close double white dwarf binaries with periods of roughly 100 sec and longer ; and a large number of unknown W UMa binaries with periods near 10^4 sec. For impulsive sources, the sensitivity would be sufficient to see pulses from the formation of black holes of 10^4 to 10^8 solar mass at large redshifts, if such events occured in most galaxies. Some useful information on a possible stochastic back-ground also could be obtained, despite having only one antenna, provided that the spectrum is quite different from that expected for spurious accelerations of the test masses and other disturbances in the system.

Two other possible antenna geometries for extending the observable period range also have been considered. One uses spacecraft at the L1, L4 and L5 points of the earth-sun system, and therefore a 1.5×10^8 km separation. This would make possible much better performance for periods longer than 10^4 sec, but with worse performance below 10^3 sec period. Additional care would be needed in the optical design because of the 2×10^4 times weaker laser power that would be received. However, it would not be necessary to measure to as small a fraction of a wavelength. Therefore, thermal distortion in the optical system, laser beam direction variations, and mirror irregularity effects would be less severe. The other geometry consists of three spacecraft 90° apart in geosynchronous earth orbits, giving 60 000 km arm lengths. In this case the performance for periods of 0.1 to 10 sec would be improved. However, performance for periods longer than about 3 000 sec would be considerably worse. Thermal disturbances and certain other perturbations also would be worse.

TREAK CAMERA-BASED LASER RANGING RECEIVER DEVELOPMENT

J.B. Abshire, J.F. McGarry, H.E. Rowe, J.J. Degnan
Instrument Electro-Optics Branch
NASA Goddard Space Flight Center
Greenbelt, MD 20771 USA

Telephone (301) 344 7000
TWX 710 828 9716

ABSTRACT

A laser ranging (LR) system which uses a 2 psec resolution streak camera (SC) receiver has been designed and constructed. The system features a 48 nsec imaging optical delay path to compensate for the trigger delay of the SC and utilizes an amplified photomultiplier (PMT) as the SC trigger detector. The system transmitter is a modelocked Nd:YAG laser which emits 30 psec pulses at 1064, 532 and 355 nm. Pulsed two-color ranging tests with this system show differential ranging accuracies of +-0.5 mm after the 355 and 532 nm pulse traverse a 921 m round trip horizontal path.

Initial SC sweep speed calibration has utilized an etalon, and the results show SC sweep nonlinearities of 8 percent. Sensitivity measurements show a minimum detectable signal of ~ 125 photoelectrons (PE) at 532 nm. This can be enhanced to the single PE level by adding an image intensifier to the system.

INTRODUCTION:

Present laser ranging (LR) systems which use modelocked laser transmitters, MCP-based PMT's, high speed preamplifiers, and low time-walk discriminators, can achieve 1 cm range accuracy (Ref. 1). For much higher accuracies, substantial improvements in receiver bandwidth must be made. Such an improvement is readily available in streak cameras which have psec time resolution. For such devices to achieve mm-level accuracies in LR systems, they must be carefully calibrated and interfaced to the ranging system. This paper reviews recent work to achieve these goals at NASA-Goddard.

The operation of a typical linear scan SC is shown in Fig. 1. The incident optical pulse illuminates the photocathode and frees photoelectrons from its rear surface. These are accelerated rapidly by a mesh electrode and then are deflected vertically by a fast electrical sweep. This results in a time-to-space mapping of the electron stream. The resulting electron distribution impinges on the microchannel plate, which preserves the spatial distribution and amplifies it. The amplified electron bundle exits the rear of the plate, and is accelerated into a phosphor screen. This produces a weak optical image whose spatial intensity distribution is proportional to the temporal intensity distribution of the illuminating optical pulse. In most streak cameras, an intensified video camera reads out this image and a OMA system converts it back to an intensity versus time profile. The phosphor image from a exponentially decaying set of optical pulses is shown at the bottom of the figure, along with the intensity versus time profile.

Circular scan SC's also have been developed for LR applications (Ref. 2). However dual channel linear-scan SC are presently favored at Goddard since they will record extended optical signals in both channels. This capability is important for sea state, altimetry, and pressure measuring applications (Ref. 3-5).

CURRENT DEVELOPMENTS:

The optical configuration of our present laboratory system is shown in Fig. 2, and its parameters are summarized in Table 1. This system operates in the following manner. The 30 psec pulses from the dye-modelocked ND:YAG laser first enter the transmit beam aligner system, which matches the divergence angles and center points of the 355 and 532 nm beams. The original offset is caused by the angle tuned KD*P doubler and tripler inside the laser. The aligned beams then are reflected up into the periscope system, and are directed to the target cube-corner (CC) by the roof periscope mirror. The optical return from the CC is reflected by the roof mirror and is collected by the receiver telescope. It is reimaged by an eyepiece, which relays the focal point to the start of the optical delay system. Just before this point, a beamsplitter reflects ∿8 percent of the optical signal into a PMT, whose output is then amplified and triggers the SC. The remainder of the energy enters the imaging delay line, which operates in the same manner as a White cell. The signal from this system then enters a light-tight enclosure, where the 355 nm pulses are reflected from a dichroic beam splitter, while the 532 pulses pass through it. The pulses in each path then pass through a bandpass filter for background light rejection. They are then recombined by a second dichroic and are focussed onto the SC photocathode.

The characteristics of the horizontal path which is currently used for 2-color ranging tests are summarized in Table 2. The 1 inch CC is mounted on a water tower, and the path passes over parking lots and buildings. Owens' 1967 refractivity formula is used to predict the refractive delay difference between the 532 and 355 nm pulses. The wavelength dependence of the refractive delay under standard atmospheric conditions is shown in Fig. 3. The meteorological data for this formula is taken from P, T, & Rh sensors mounted at the periscope mirror. Sensor accuracy is sufficient to allow less than 1 psec uncertainty in differential delay over this short path.

Laser pulse shapes recorded by the system are shown in Fig. 4. The left hand pulses were recorded from the reference path, while the right hand pulses were recorded after a second pulse pair traversed the horizontal path. The pulses are correctly aligned in time for both figures. The shift of the 355 nm pulse in the right hand pair is caused by the additional refractive delay it encounters in the path. The small scale structure within the pulses shows the psec temporal resolution capability of the SC system.

A typical output of the computer program which processes the SC data for dispersion measurements is shown in Fig. 5. Recorded waveforms at 532 & 355 nm are shown on the left hand side, while the convolution of the two is shown at the top right. For every laser firing, the program selects the peak of the convolution as its best estimate of the differential delay. The bottom figure right shows the histogram of the differential delay values. The mean and standard deviation of the differential delay are calculated from this histogram. Here, one channel corresponds to 2.2 psec.

To achieve accurate timing, the streak camera time base must be accurately calibrated. This is done by inserting a lossy etalon into the reference path, as is shown in Fig. 6. A single pulse input into the etalon results in a train of pulses with exponentially decaying intensities. These pulses are separated by the etalon round trip time. Since this time is accurately known by the setting of the translation stage, the pulses can be used as calibration markers.

A typical output from the calibration computer program is shown in Fig. 7. The upper left waveform shows the raw 532 nm data from a single laser firing as recorded by the SC. For this data, the etalon was aligned to emit only two pulses into the system. The upper right waveform shows the raw data after being convolved with a 25 channel-wide raised cosine impulse response.

The peak x-values from each pulse is then recorded. After multiple laser firings, the computer calculates the average value of the first peak x-value and the x-separation. The sweep speed profile can be measured by repeating this procedure after changing the x-value of the first peak.

The results of this procedure are shown in Fig. 8. Each point plotted here is the average of approximately 25 measurements, and the error bars are the standard deviation of the sample mean values. The data show that the sweep speed is fastest at the start of the sweep, and slows by ∿8 percent over the region shown.

To calculate the atmospheric delay, the fixed offsets within the LR system also must be removed. This is done by first measuring the differential delay over the horizontal path. Then the laser output is blocked from traversing the path and the reference shutter is opened. The same procedure is then repeated while the laser pulses traverse only the reference path. Since all fixed offsets within the system are common to both paths, subtracting the reference values from the path values leaves only differential delay caused by the atmosphere. Both the sweep speed and offset corrections are very similar to those developed for a waveform digitizer-based two color LR system (Ref. 6).

Results from repetitively measuring the atmospheric dispersive delay after using these procedures are shown in Fig. 9. Each plotted point is the mean value of 25 measurements while the error bars show +- one standard deviation. The average bias of the first set of 4 points is -3 psec, while the average bias of the second set of 9 points is ∿2 psec. The shifts in the average values are thought to be caused by small errors in spatially aligning the reference to the tower path. Even with these errors, the differential ranging accuracy is within +-0.5 mm for this measurement set. This data shows the very high LR accuracy which is available with SC-based receivers.

FUTURE DEVELOPMENTS:

SC technology also can be used in an "optical time-interval-unit" (OTIU). This devices utilizes the high time resolution of the SC for its optical interpolator. A "coarse" 500 MHz electronic counter is used to measure the integer number of clock pulses between the incoming optical start and stop pulses. Such an approach based upon our existing SC technology is shown in Fig. 10. This approach is somewhat similar to our earlier one for circular-scan SC's (Ref. 2), but uses optical clock pulses. In the present design, both the start and stop laser pulses are detected by the PMT, which triggers both the electronic TIU and the SC. Most of the optical pulse energy is directed into the optical delay line for recording by the SC. Short optical pulses which are coincident with the TIU clock are generated by a several GHz bandwidth laser diode within the optical clock module. These are optically summed with the laser pulses into the SC optical input. Both the SC and TIU output digitized data into the computer for each start/stop laser pair.

The principle of a two-color OTIU operation is shown in Fig. 11. In the left column, both the SC image and the optical waveforms are shown for the start pulse. In this representation, both laser colors are shown to be coincident in time. Therefore only the time interval between the first clock pulse and the laser pulse must be recorded. The right column shows the same data for the stop pulse. For this return, the two-color pulses have been temporally separated by the atmosphere. Therefore the computer must calculate the differential arrival time between pulses as well as the single color delay at wavelength 1. Given this data, it is straitforward to calculate the single color delay and the atmospheric correction by using the formulas shown. Such a system is presently being constructed by the authors.

SUMMARY:

SC-based laser ranging receivers are currently being developed at NASA-Goddard. Test results show that when systematic errors are properly controlled, differential range accuracies of +-0.5mm are readily achievable. Higher accuracies should be possible with more work. The accuracies already achieved exceed those typical of state-of-the-art PMT-based receivers by an order of magnitude. Such SC-based systems can be used to measure single color atmospheric delays to 5mm using two-color ranging. They also can be used to construct complete ranging receivers with accuracies of a mm or better.

ACKNOWLEDGEMENT:

We would like to thank Kent D. Christian for his technical assistance in operating the SC system.

REFERENCES:

1. J. J. Degnan, T. W. Zagwodzki, H. E. Rowe, "Satellite Laser Ranging Experiments With an Upgraded Moblas Station," this proceedings.
2. C. B. Johnson, S. Kevin, J. Bebris, and J. B. Abshire, Applied Optics, Volume 19, 3491 (1980).
3. C. S. Gardner, B. M. Tsai, and K. E. Irw, Applied Optics, Volume 22, 2571 (1983).
4. J. B. Abshire and J. E. Kalshoven, Jr., Applied Optics, Volume 22, 2578 (1983).
5. J. B. Abshire, J. F. McGarry, B. M. Tsai, and C. S. Gardner, Conference on Lasers and Electro-Optics, Paper WL2, Anaheim CA, June 1984.
6. J. B. Abshire, "Pulsed Multiwavelength Laser Ranging System," NASA Technical Memo 83917, March 1982

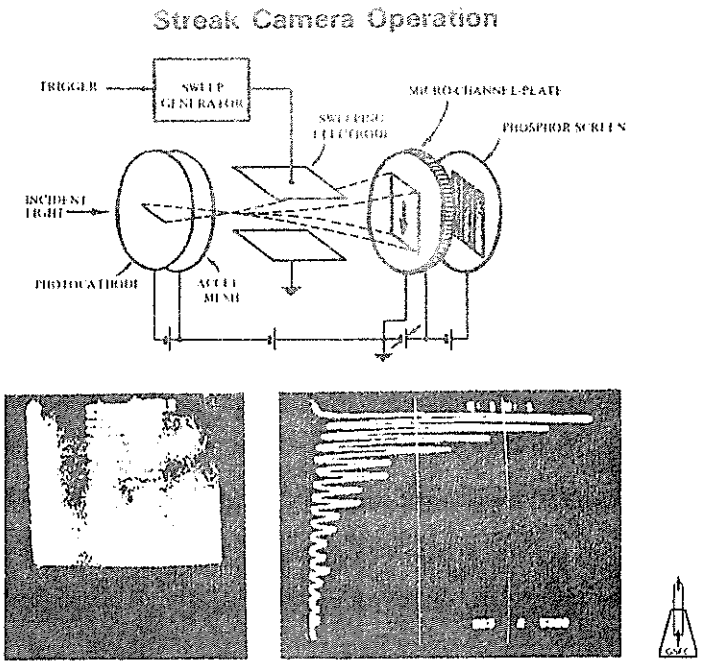

Figure 1 - Streak Camera Operation

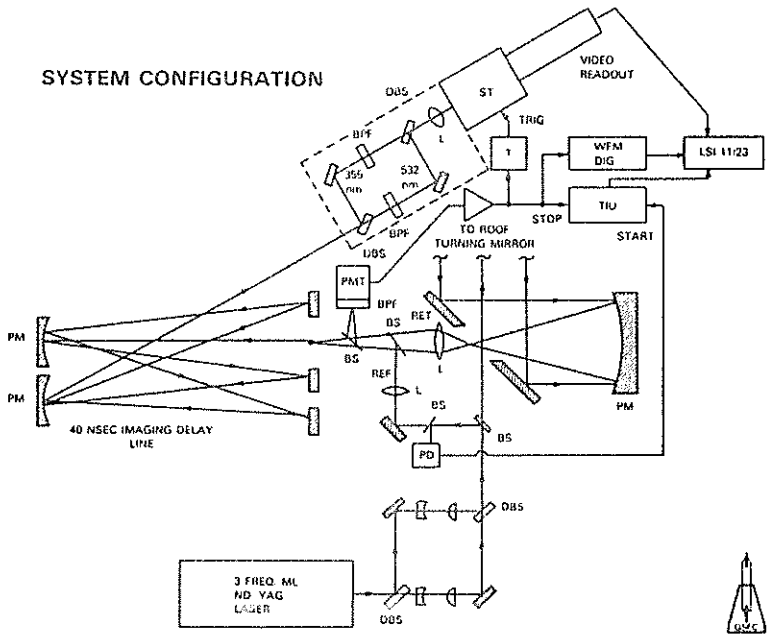

Figure 2 - Present Streak Camera-Based Ranging System

STREAK CAMERA-BASED RANGING SYSTEM PARAMETERS

LASER	QUANTEL YG 40 dye ml, 30 psec FWHM 5 mJ @ 1064 nm, 2 mJ @ 532 nm, 1 mJ @ 355 nm DIV 0.3 TO 1.0 mrad, align: <10% DIV
MIRRORS	Double dielectric, MAX R @ 355 & 532 nm
T_{sys}	Typ 45% AT 532 & 355 nm, (excluding telescope & periscope)
TELESCOPE	460 cm^2 AREA, 91 cm FL
PMT	HAM R1294, MCP type, QE ~ 4%, G ≈ 10^5
WAVEFORM DIGITIZER	TEKTRONIX R7912
TIU	HP5370, 100 psec accuracy
STREAK CAMERA	HAM 1370, 2 psec resol., 550 psec window, 2.2 psec/chan
MINICOMPUTER	DEC LSI 11/23, SKYMNK array proc., dual floppy disks

Table 1 - Streak Camera System Parameters

TWO COLOR RANGING TEST PATH

LENGTH	:	921.2 m (round-trip)
ELEVATION ANGLE	:	+3.5 deg
REFLECTOR	:	2.54 cm CC
END POINT SENSORS	:	T — aspirated thermometer P — setra 270 Rh — hair hygrometer
ALGORITHM	:	$\Delta T_{32} = \frac{L}{c} \Delta r_{g32} (P_m, T, Rh)$ $L = cT_2 [1 - r_{g2} (P_m, T, Rh)]$ $r_{g\lambda} (P_m, T, Rh) \equiv$ group refractivity at λ (OWENS, APP. OPT., 1967) P_m — midpoint pressure T_2 — TIU reading at λ_2

Table 2 - Horizontal Path Used for Ranging Tests

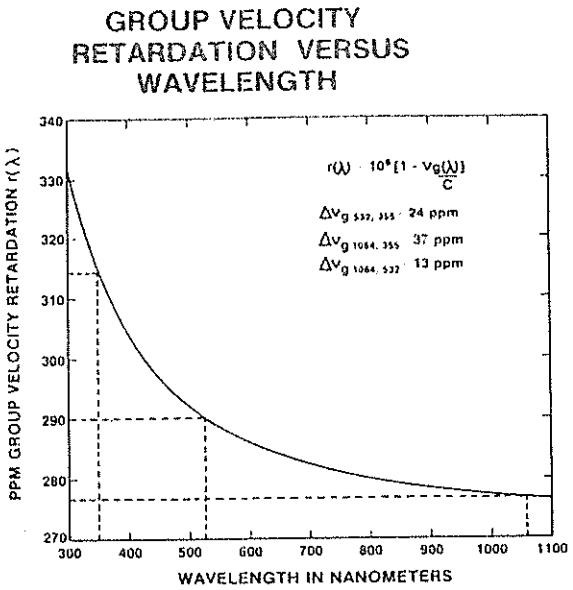

Figure 3 - Group Velocity Dispersion of Air Under Standard Conditions

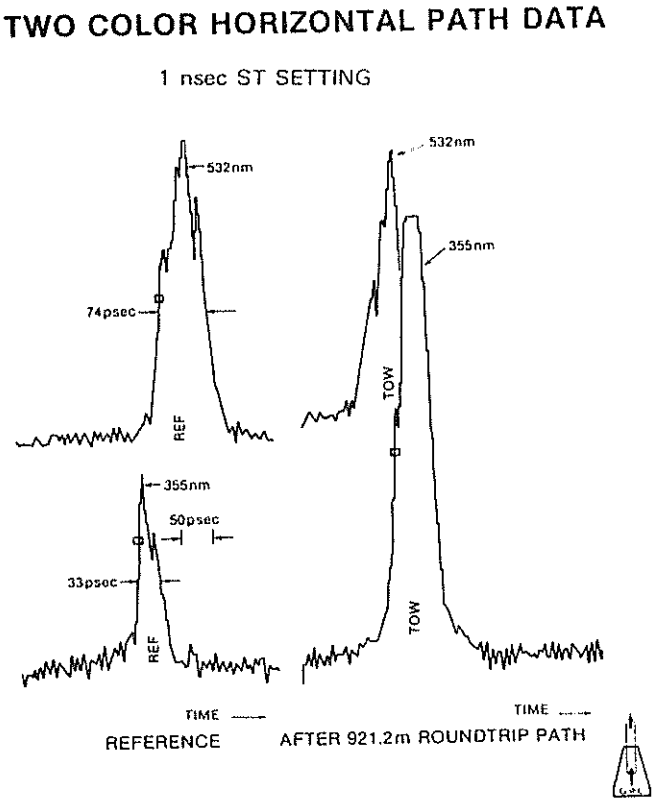

Figure 4 - Optical Pulse Shapes Recorded by Streak Camera Receiver System

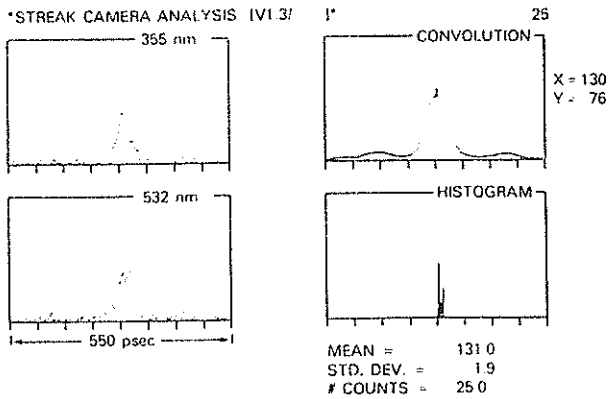

Figure 5 - Typical SC Computer Analysis

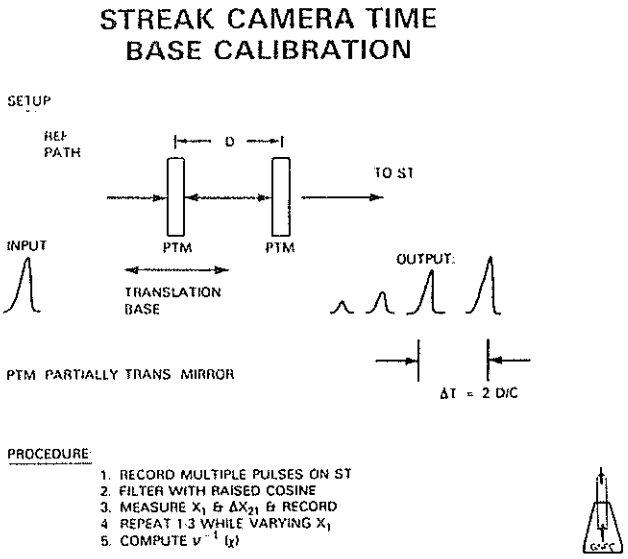

Figure 6 - Calibration Procedure for the SC Time Base

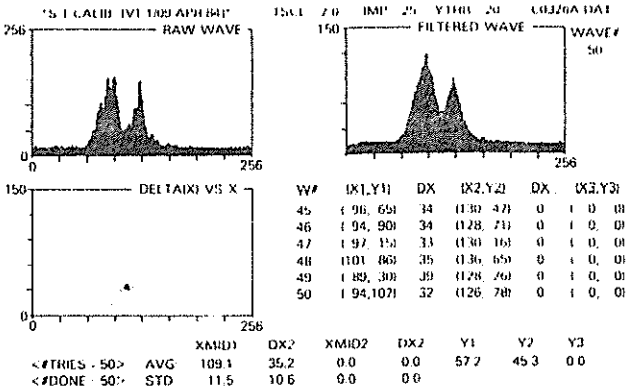

Figure 7 - Typical Output of SC Time Base Calibration Program

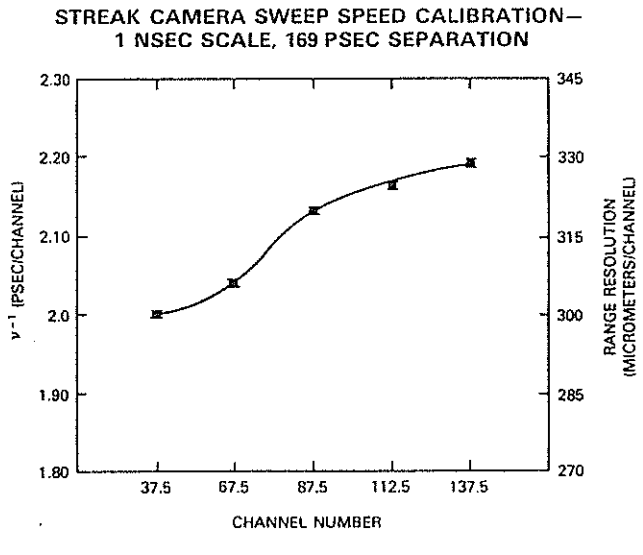

Figure 8 - SC Sweep Speed Profile

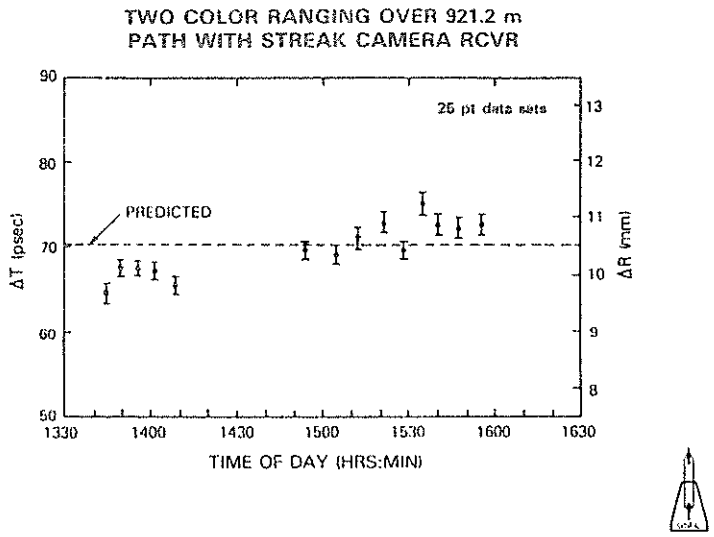

Figure 9 - Two Color Ranging Results Using SC Based Receiver

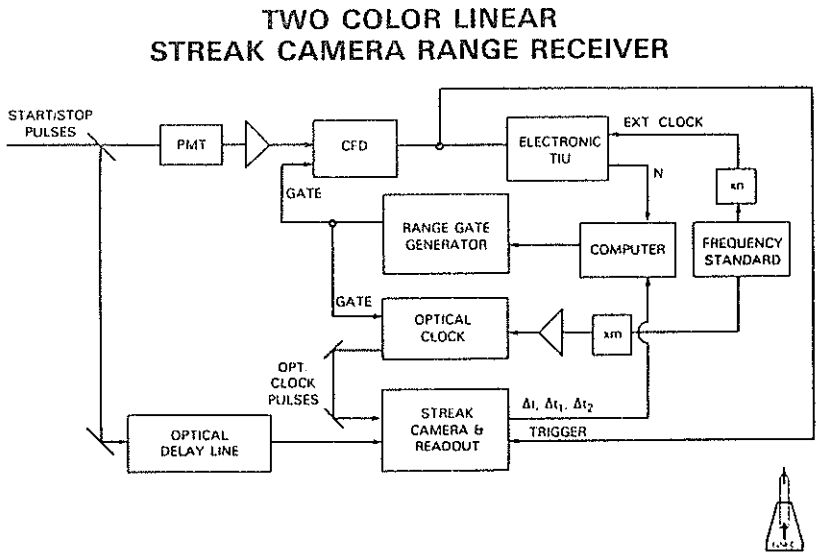

Figure 10 - SC Based Optical Time Interval Unit

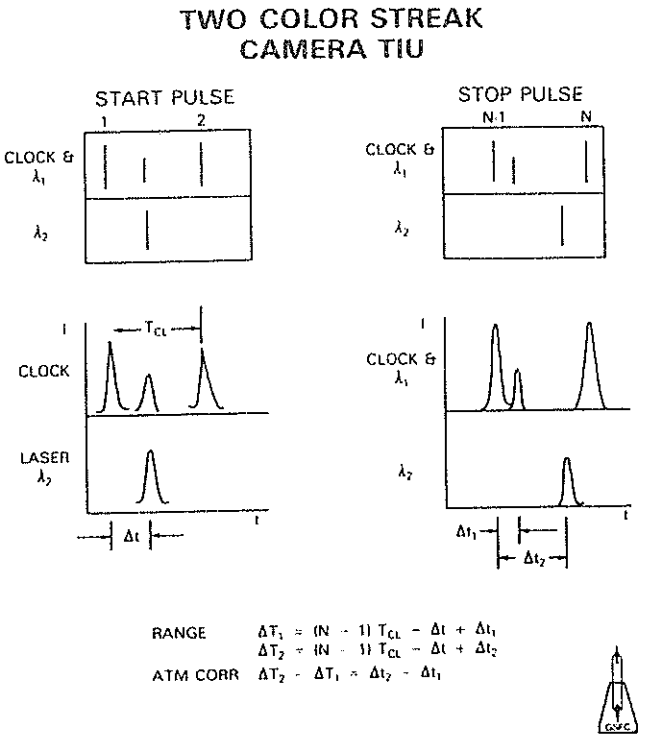

Figure 11 - Start and Stop Sweeps of Optical Time Interval Unit

NEW LASER DEVELOPMENTS TOWARD A CENTIMETER ACCURACY LUNAR RANGING SYSTEM

S.R. Bowman, C.O. Alley, J.J. Degnan*
W.L. Cao**, M.Z. Zhang**, N.H. Wang**
Dept. of Physics and Astronomy
University of Maryland
College Park, Maryland 20742 USA

Telephone (301) 454 3405
Telex 908787

*Now at Goddard Space Flight Center of the National Aeronautics and Space Administration

**Visiting Scholars from the Shangahai Institute of Optics and Fine Mechanics Academica Sinica, P.R.C.

ABSTRACT

The design considerations and performance characteristics of the currently operating laser are briefly described. The laser was designed and constructed for the specific purpose of lunar ranging.

Our goal is the establishment of a high accuracy lunar ranging station at the 48-inch Precision Tracking Telescope located on the Goddard Optical Research Facility in Greenbelt, Maryland. This paper describes the laser system designed and built to be the transmitter for this station.

Losses in the atmosphere and telescope were a major concern in the ranging system design. To overcome these losses we pressed the laser design for high average power. Of course, short pulse length, low output divergence, and reliability could not be compromised. Eventually, a mode-locked Neodymium YAG laser configuration emerged which we feel should give acceptable signal strength. The optical layout and output parameters are given in Fig.1.

The heart of a laser system is the oscillator. Our oscillator design emphasizes maximum output energy in a single, gaussian spatial mode pulse. This reduces the number of amplifiers needed thereby simplifying the overall system. A polarization switch cavity dump gives a factor of at least three improvement in energy compared to external pulse selectors. A combination of active mode-locking with an acousto-optic modulator and passive Q-switching with a nanosecond recovery dye (Kodak 14617 dye in dichloro-ethane) produced the 100 picosecond pulse length we wanted.[1,2] Simple passive mode-locking and etalon pulse stretching techniques did not allow stable Q-switching at higher energies.

Damage in the flowing Q-switch dye cell was the most difficult problem we encountered. We now believe it was due to absorptive heating near the dye cell windows. The problem was overcome by using a large transmission dye cell near the cavity center which slowly translates perpendicular to the beam.

The oscillator now delivers 800 to 1000 microjoules in a single, "S" polarized pulse. The transverse mode is TEM_{oo} and the energy stability is 5 to 10 percent. The half power pulse duration is 107 picoseconds as measured by a picosecond resolution Hadland Photonics streak camera.

After the oscillator, we have two high gain laser amplifiers. Two amplifiers are required to get the energy up near the damage threshold, because of the onset of amplified spontaneous emission when the gain becomes too high.

Fig. 1 Goddard/Maryland Lunar Ranging System
Laser Transmitter

Output Parameters:

- Single pulses at 10 Hertz
- Pulse duration 107 picoseconds
- Pulse energy 0.52 Joules @ 1064nm
  0.31 Joules @ 532nm
- Beam divergence less than 200 microradians
- Polarization 98% "P" @ 1064nm

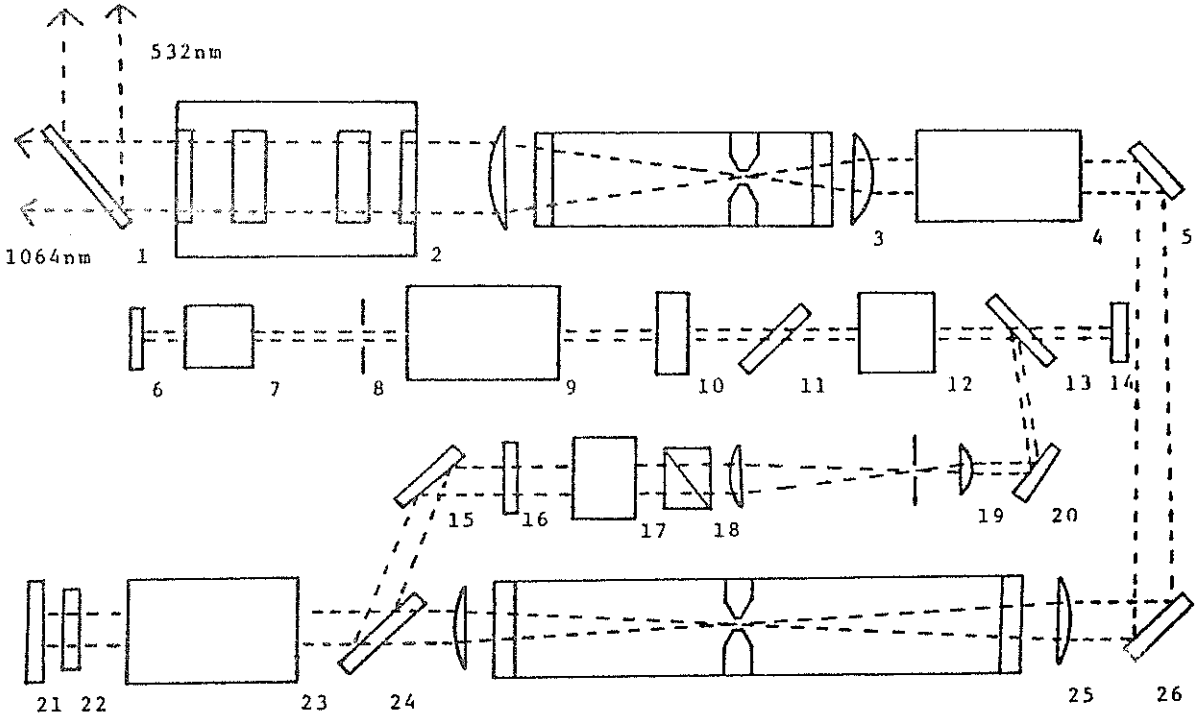

1 - 45° dichroic beamsplitter
2 - Two crystal harmonic generator
3 - F/20 vacuum spatial filter
4 - Nd:YAG amplifier (9 mm diameter)
5,26 - 45° HR mirrors
6 - Normal incidence HR mirror (10m curvature)
7 - Acoustooptic modulator
8 - Mode selection aperature
9 - Nd:YAG oscillator head (3mm diameter)
10 - Flowing saturable dye cell
11,13,15,24 - Multi-layer dielectric polarizers
12,17 - Pockels cells
14,21 - Normal incidence HR mirrors (flat)
16 - Half wave plate
18 - Glan-Thompson polarizer
19 - F/50 spatial filter
20 - 33° HR mirror
22 - Quarter wave plate
23 - Nd:YAG amplifier (7mm diameter)
25 - F/50 vacuum spatial filter

Separating components in the amplifier chain, there are three spatial filters. These increase the system's average power in a number of ways:[3,4]

i) reduced damage caused by the growth of high spatial frequency intensity components;
ii) reduced damage from diffraction ripple by image relaying;
iii) increased energy from amplifiers by efficient filling of laser rods;
iv) increased firing rate by correcting for thermal lensing of laser rods;
v) increased isolation between amplifiers allows higher gain.

Infrared output of the laser system is 520 millijoules per pulse with pre-pulse energy of less than one millijoule. At 10 Hertz firing rate the output beam is 98 percent "P" polarized with less than two times diffraction limited divergence.

The 532 nanometer second harmonic is generated with a KD*P type II, angle tuned crystal. The crystal is 15 millimeter long and immersed in a temperature stabilized, index matching fluid. The last spatial filter expands the beam so that the intensity on the doubler is 2×10^9 watts/cm^2. Present doubling efficiency is a somewhat disappointing 45 percent. Single crystal doubling efficiencies as high as 74 percent have been reported in the literature and we are still working to improve our number.

In addition to the single crystal second harmonic work, we have tested one of several two crystal doubling techniques.[5,6] Two KDP type II crystals have been used in a quadrature scheme to generate 60 percent conversion efficiency. Some practical problems remain to be solved and we are continuing this work.

The Maryland/Goddard Lunar Ranging Station was activated briefly in the fall of 1984. Ranging results from LAGEOS at that time uncovered some minor problems in the system. At the time of this writing (January, 1985), those problems have been solved and the station is about to resume operation.

An additional amplifier with slab geometry is being designed to increase the output energy further. It utilizes recently available large size neodymium doped YAG material and will probably utilize an active mirror configuration.

References

1. W. Seka and J. Bunkenburg, J. Appl. Phys. 49, 2277 (1978).
2. G. A. Reynolds and K. H. Drexhage, J. Appl. Phys. 46, 4852 (1975).
3. J. T. Hunt, J. A. Glaze, W. W.Simmons, and P. A. Renard, Appl. Opt. 13, 2053 (1978).
4. J. Holzrichter, "High-power pulsed lasers," Lawrence Livermore Laboratory Internal Report UCRL-52868 (April 1980).
5. V. D. Volosov, A. G. Kalintsev, and V. N. Krylov, Sov. J. Quantum Electronics 6, 1163 (1976).
6. G. J. Linford et al., Appl. Opt. 21, 3633 (1982).

PROGRAMMING FOR INTERLEAVED LASER RANGING

J.D. Rayner
Dept. of Physics and Astronomy
University of Maryland
College Park, Maryland 20742 USA

Telephone (301) 454 3405
Telex 908787

ABSTRACT

The use of epoch timing and multi-tasking in the University of Maryland Lunar Ranging System is described with emphasis on the problems created by interleaved starts and stops.

The only significant difference between programming for lunar and for satellite ranging is that in the lunar case, the time between laser shots is considerably less than the round trip time to the target. This complicates the timing since we now have many interleaved start pulses between corresponding start and stop pulses. In this situation a single time interval meter is no longer sufficient. One way to deal with this problem is to measure independently the epoch of the outgoing and returned pulses. The round trip time can then be derived by simple subtraction.

Although this is the chief reason to go to epoch timing there are several other advantages to be gained by incorporating an epoch timer in a ranging system. Among these are:

1) The epoch timer serves as the station time of day clock,

2) It can directly measure the station epoch,

3) It can generate a return gate for the received pulse,

4) The laser firing epoch is automatically measured to high accuracy.

Although use of a multi-tasking operating system is desirable for any ranging system, it is particularly valuable for one based on epoch timing and almost indispensable for one with interleaved starts and stops. The key feature of a multi-tasking operating system is its ability to run many programs at the same time. This is accomplished by switching control of the computer between the various competing programs. Use of a multi-tasking system allows the ranging program to be separated into pieces without regard to the details of timing. These pieces or tasks are then synchronized by exchanging messages between themselves. For example, a data collection task can send a message to a data output task saying "I have some data for you to write to disk". The output task then starts up and writes the data out.

The partitioning of a multi-tasking program into its various tasks is one of the key decisions in the design process. The partitioning of the Maryland ranging program is shown in Figure 1. As the figure shows, the program consists of four tasks. The range task calculates the range to the moon once a second. It is synchronized to the real world by a message sent once a second by the epoch timer control task. On receiving the message it makes the range and range rate available to the event timer control task in a buffer. The display task runs at the lowest priority using whatever time is not used by more important tasks to plot a histogram of as many range residuals as possible. It sets a flag when it is ready to process a point, then the data from the next

return is sent as a message by the epoch timer control task. As range data is acquired it is sent to the output task. Then when a buffer fills up, the output task writes it to disk.

This leaves the epoch timer control task which is the heart of the system. This is really a collection of tasks all executing the same code. Three different structures were considered. We could have had one task devoted to the epoch timer which then decides whether the next measurement is a stop or start. An alternative to this is to have two tasks one for starts and one for stops. You then need a scheduler to decide which task to activate next. Our system uses a third approach, with each shot handled by a separate task which measures the start epoch then goes dormant until it is time to take care of the stop. The actual code for the three different approaches is quite similar, in that they all need to schedule the epoch timer. The third method was chosen because arranging the code sequentially for one shot seemed conceptually simpler. At a 10 pps repetition rate we have about 25 invocations of the epoch timer control task running. Of course all but one are dormant, waiting for their turn at the epoch timer program. Each task uses the same copy of the Event Timer Program, but each has its own data block in which it keeps its own local data.

The key to the program is the scheduling of the epoch timer which is handled by the scheduler sub-routine. The scheduler maintains two lists or queues of data blocks, one for starts and one for stops. The epoch timer control program gives the scheduler a data block and a pointer to the appropriate queue. The block is then linked to the end of the indicated queue and the calling task is suspended. When the epoch timer finishes measuring the time of a start or stop it is necessary to determine the next task to use the epoch timer. Each data block contains the expected time for its associated start or stop. Therefore, it is just a matter of comparing the times contained in the data blocks heading the two queues and scheduling the one with the earliest time. If the the times are within 1 millisecond of each other, the stop task is aborted and the start task scheduled, since the laser firing would wipe out any return.

By using an epoch timer and a standard multi-tasking operating system we were able to generalize our non-interleaved satellite ranging progam to the interleaved lunar ranging case with a minimial amount of trouble using many pieces of the satellite program.

TASK STRUCTURE

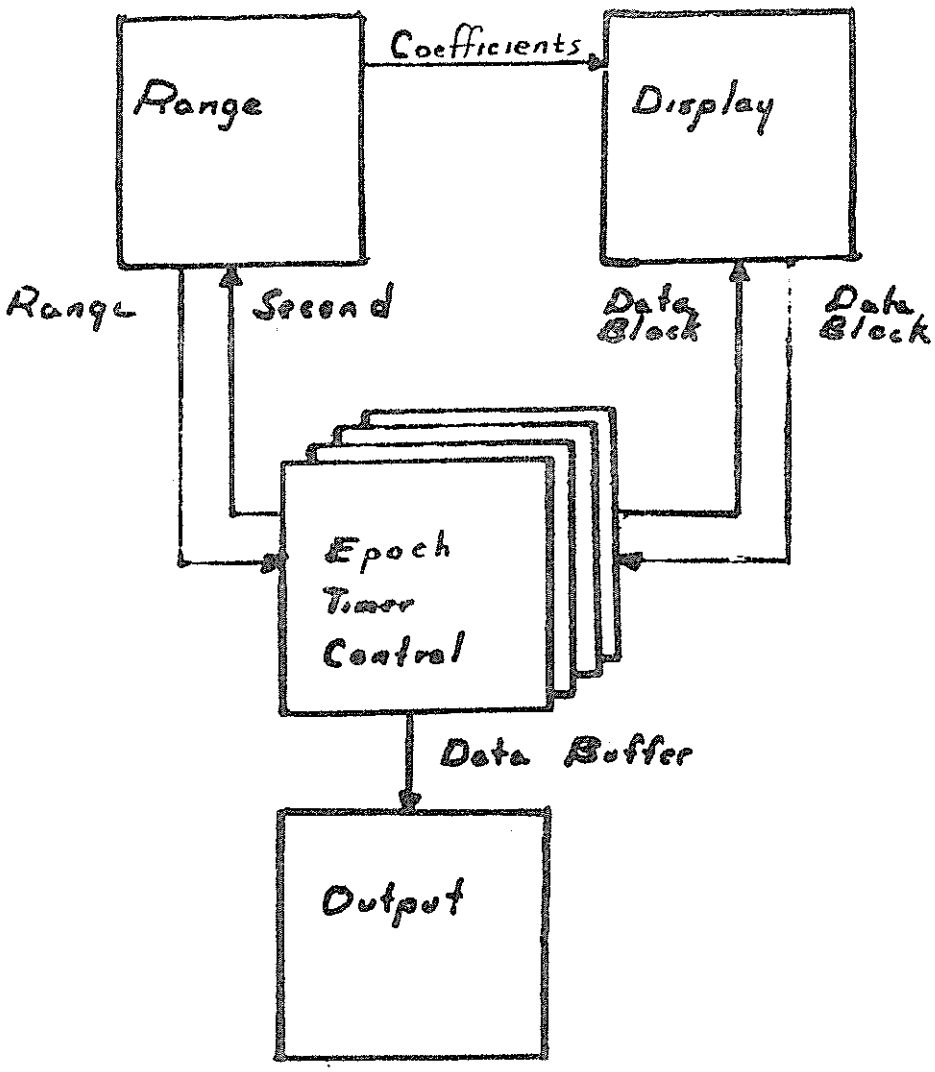

FIGURE 1

PERFORMANCE OF SATELLITE LASER RANGING DURING MERIT

B.E. Schutz, B.D. Tapley, R.J. Eanes
Center for Space Research
The University of Texas at Austin
Austin, TX 78712 USA

Telephone (512) 471 5573
Telex 7044265

ABSTRACT

Over 30 stations contributed data to the MERIT Project, with some stations operating at the 1-2 cm single range measurement level of precision. Thes stations tracked over 5000 LAGEOS Passes and over 2500 STARLETTE passes during the 14 month campaing, an average of over 10 passes per day for LAGEOS. Rapid service earth rotation solutions were possible because of the timely availability of the data. Improvements in the models used for the analysis of the data have enabled identification of instrumental anomalies at the 20 cm level in range bias and 150 microsecond level in time bias.

PERFORMANCE OF SATELLITE LASER RANGING DURING MERIT

Introduction

Since the Fourth Laser Ranging Workshop in October 1981, numerous developments in applications to artificial satellites have occurred. These developments include the introduction of new mobile satellite laser ranging (SLR) systems, the introduction of improved hardware in existing systems, and the addition of new stationary systems. Although some aspects of the developments can be regarded as the result of the SLR evolutionary process, most of the developments have been motivated by the NASA Crustal Dynamics Project and the IAU/IUGG project to monitor earth rotation and intercompare the techniques (MERIT).

This paper summarizes the performance of SLR systems in the MERIT period (September 1, 1983, to October 31, 1984) and contrasts the performance to the pre-MERIT period. The performance is characterized in terms of tracked passes, estimated instrument precision and number of participating sites. Because of improvements that have been possible as the result of improved instrument performance, concommitant improvements have been possible in the satellite force models, measurement models and kinematic models. These latter improvements have produced analysis techniques that enable identification of instrumental errors in near real-time at levels of 20 cm in range bias and 150 microseconds in time bias.

Data Sets

The results have been obtained using full-rate (FR) and quick-look (QL) data. The QL data are sampled at approximately 50 points per pass and are transmitted within a few hours after acquistiion via telex, GE Mark 3, computer modem or other means of data communication. The FR data, on the other hand, encompass the complete set of data and are usually transmitted from the respective station via magnetic tape to a Data Collection Facility (DCC). During the MERIT period, the DCC for QL and FR data has been located at the Goddard Space Flight Center (GSFC).

The pulse repetition rate now used with new laser systems is sufficiently high that some passes exceed 10,000 full-rate LAGEOS range measurements at a single station. To reduce the computer time required for data analysis while retaining the information content of the individual measurements, a data compression technique has been used to create normal points (NP). The LAGEOS normal points used in this paper were created from bins of raw data spanning three minutes. The technique used is essentially "Recommendation 84A: SLR Normal Point Generation and Exchange," differing only by the compression window (three minutes versus the recommended two minutes). STARLETTE normal points have been formed using 30-second bins.

Analysis Procedures

The analysis of laser range data is performed on a regular basis at the Center for Space Research. Quick-look data are received in a PDP 11/60 computer via a computer modem, and the received files are merged and preprocessed. The data are translated into the Modified Seasat Decimal format and transferred electronically via a dedicated circuit to The University of Texas academic computing facility for further processing on the dual CDC Cyber 170/750 computers. The accumulated data are processed each Tuesday for the earth rotation solutions which are then placed on the GE Mark 3 system. Since May 1984, the earth rotation solutions have been performed using normal points formed from the QL data. The formation of the normal points provides an initial level of data editing through computation of a preliminary earth rotation solution based on the raw QL data. The range residuals resulting from this solution are further analyzed and edited to create QL normal points. The resulting normal points are used in the final earth rotation solutions reported on Mark 3 as ERP (CSR) 84 L 02. The reported solutions include both "final" and "preliminary" solutions, where the latter case represents an incomplete five-day interval or that additional data are expected. In addition, unreported solutions are made based on all available data, however, these solutions may span only one or two days. Both the preliminary and the unreported solutions provide a near real-time opportunity to assess the current data quality and to aid in the identification of anomalous station performance. These basic procedures have been in use since the short MERIT Campaign in 1980.

In addition to the weekly assessment, a somewhat more formal process is performed on a monthly basis for LAGEOS. This analysis is distributed in a monthly report of the Center for Space Research, "Analysis of LAGEOS Laser Range Data," prepared with the support of NASA. The monthly report provides detailed information on the stations used in the earth rotation solutions and provides additional information on individual station performance. The station performance is summarized through the use of a single, continuous orbital arc spanning at least one month. This arc is fit to the unedited QL data for the purpose of providing detailed analysis of station performance, computing final QL normal points and incorporating data into the data base that was received too late for the weekly earth rotation solutions. The force and kinematic model used for the long-arc orbit computations in UTOPIA (Schutz, et al., 1982) is essentially consistent with the MERIT Standards (Melbourne, et al., 1983). Because of small errors in these models, the least squares estimation process is unable to fit the data to the measurement noise. Nevertheless, these model errors normally have unique signatures when compared with the instrumental error sources discussed by Pearlman (1984). Further information on the analysis procedures is given by Tapley, et al. (1981).

Performance

International tracking campaigns such as MERIT have made significant contributions to the performance of laser systems. Such campaigns have encouraged the development of improved systems, promoted the

development of new systems and fostered international cooperation. The growth in laser ranging activities from operational systems capable of tracking LAGEOS is reflected in the number of full-rate passes tracked in each five-day interval since May 8, 1976, until September 30, 1984. This feature is shown in Figure 1. The steady increase during the Main MERIT Campaign is readily apparent, in part because of the participation during the Intense Campaign during April-June, 1984. It is also apparent that more passes of LAGEOS were obtained during MERIT than during any other comparable period.

Before the MERIT Campaign was completed, 20 stations had provided data during a single 5-day period (earth rotation epoch 26 October 1984), a remarkable change from the number of stations contributing in 1981 (typically, 4 to 6). The individual pass contributions of each station during MERIT are shown in Table 1 for LAGEOS and STARLETTE. Additional information on the individual station hardware characteristics are given by Schutz (1983).

The monthly assessment of station performance using the previously described procedures generally results in range residuals with an overall RMS of 10-12 cm. In this assessment, all range measurements are equally weighted except for those stations with known systematic problems or new stations with significantly uncertain station coordinates. As a consequence, the resulting RMS is indicative of remaining force and kinematic model errors as well as possible instrumental problems. Through the process described by Tapley, et al. (1982), the range residuals in a pass can be resolved into "range bias" and "time bias." After removal of the range bias and time bias, the remaining systematic trends in the residuals can be removed by appropriate polynomials, and an estimate of the instrument precision can be made from the resulting residuals. As an indication of current performance in quick-look (QL) and full-rate (FR) data, Tables 2 and 3 illustrate the precision estimates for August 1984. It is evident from these tables that the precision of raw QL and FR data is comparable and ranges from 1-2 cm for some stations to tens of centimeters for others. Because the edit criteria generally used is about 30 cm, the data are significantly edited from stations which operate with precision greater than 20 cm.

It is the general guideline that about 50 points of QL data be transmitted per LAGEOS pass; however, as noted previously, some stations obtain more than 10,000 FR points in a pass. As a consequence, the normal points created from the QL and FR data have somewhat different levels of precision due to the significant difference in the number of measurements that are compressed into a single normal point. Although the selected QL points are somewhat randomly spread over the pass, judicious selection of QL points has consistently resulted in smaller QL precision than FR precision for at least one station (Simosato).

The STARLETTE station performance is summarized in Table 4. Comparison of the precision estimates in this table with the LAGEOS values in Table 2 show comparable performance.

For various reasons, the editing criteria used in the analysis of QL data generally results in an editing of 5-20 percent of the data. Further analysis of the edited data provides an indication of anomalous performance or other problems. Based on the current force and kinematic model accuracies, it is possible to resolve instrumental problems with the previously described procedures at the level of 20 cm in range bias and 150 microseconds in time bias. As a consequence, time tag errors at the millisecond or more level have been readily observed, and information has been provided to the stations regarding such an anomaly.

Because of the rapid availability of QL data, it has been possible to provide timely results of earth rotation parameters (ERP). As noted previously, the ERP from SLR have been produced weekly and made available on the GE Mark 3 System. Because of the inherent delays in making FR data available, the comparable ERP solutions have lagged the QL solutions by several months. However, comparisons between ERP results obtained from QL and FR data for the first three months of the MERIT Campaign showed differences in the x and y pole position of less than one milliarcsecond. Experience has shown that the QL data not only provide a significant data resource for the identification of anomalous instrument performance and orbit maintenance, but it is also a very useful scientific resource. To enhance the scientific usefulness, the transmittal of QL normal points, rather than selected raw ranges, is a matter that should be encouraged.

Analyses for earth rotation parameters obtained during MERIT has illustrated the high performance of the stations. Comparisons with other techniques, such as VLBI, have demonstrated consistent agreement at the 2 milliarcsecond level (Robertson, et al., 1985). Such comparisons have generally been based on the QL results of SLR data, thereby emphasizing the significant scientific importance of QL data.

Conclusions

The satellite laser ranging community put forth a very strong effort during the MERIT project. Over 30 stations contributed data to the project, with some stations operating at the 1-2 cm single range measurement level of precision. Rapid service earth rotation solutions were possible because of the timely availability of data. Improvements in the models used for the analysis of the data have enabled identification of instrumental anomalies at the 20 cm level in range bias and 150 microsecond level in time bias.

Acknowledgments

The contributions of John Ries and M. K. Cheng are gratefully acknowledged. This research was supported by NASA Contract No. NAS5-27344.

References

Melbourne, W. G., R. J. Anderle, M. Feissel, R. King, D. D. McCarthy, D. E. Smith, B. D. Tapley and R. O. Vicente, Project MERIT Standards, USNO Circular No. 167, Washington, D. C., 1983.

Pearlman, M. R., "Laser System Characterization," Presented at the Fifth International Workshop on Laser Ranging," Herstmonceux, 1984.

Robertson, D. S., W. E. Carter, B. D. Tapley, B. E. Schutz and R. J. Eanes, "Polar Motion Measurements: Sub-Decimeter Accuracy Verified by Intercomparison," Science, To Appear, 1985.

Schutz, B. E. and B. D. Tapley, "UTOPIA: University of Texas Orbit Processor," Center for Space Research, The University of Texas at Austin, 1984.

Schutz, B. E., "Participants During Project MERIT," CSR-83-3, Center for Space Research, The University of Texas at Austin, 1983.

Tapley, B. D., B. E. Schutz and R. J. Eanes, "A Critical Analysis of Satellite Laser Ranging Data," Proceedings of the Fourth International Workshop on Laser Ranging, pp. 523-567, Geodetic Institute, Bonn University, 1982.

TABLE 1. MERIT QUICK-LOOK SUMMARY

Passes reported September 1, 1983, to October 31, 1984, as quick-look data (unedited)

		LAGEOS PASSES	STARLETTE PASSES
1072	Zvenigorod	21	7
1148	Ondrejov	4	53
1181	Potsdam	127	67
1873	Simeiz	33	23
1893	Crimea	7	0
7086	Ft. Davis	147	0
7090	Yaragadee	291	129
7105	Greenbelt	248	152
7109	Quincy	452	248
7110	Monument Peak	473	256
7112	Platteville	165	155
7121	Huahine	158	55
7122	Mazatlan	186	70
7210	Haleakala	389	23
7805	Metsahovi	31	2
7810	Zimmerwald	57	39
7824	San Fernando	5	3
7831	Helwan	3	3
7833	Kootwijk	72	32
7834	Wettzell	330	55
7835	Grasse	93	9
7837	Shanghai	58	0
7838	Simosato	243	141
7839	Graz	177	117
7840	Herstmonceux	339	59
7843	Orroral	42	0
7886	Quincy/TLRS-1	49	0
7907	Arequipa	432	627
7935	Dodair	13	5
7939	Matera	383	363
7940	Dionysos	3	2
8833	Kootwijk/MTLRS-1	13	1
Total		5044	2696

TABLE 2. AUGUST 1984 LAGEOS QUICK-LOOK (QL) DATA AND THREE-MINUTE NORMAL POINTS (NP)

Station	Passes	Number of QL Ranges	QL Precision (cm)	Number of NP Ranges	NP Precision (cm)
1181 Potsdam	16	417	19.8	87	8.6
7086 Ft. Davis	14	694	6.8	121	2.5
7090 Yaragadee	15	684	1.5	175	0.7
7105 Greenbelt	23	1050	2.7	228	1.2
7109 Quincy	54	2631	2.6	733	1.2
7110 Monument Peak	50	2403	2.7	544	1.2
7112 Platteville	13	332	14.9	96	7.3
7121 Huahine	6	256	8.8	53	4.0
7122 Mazatlan	14	632	6.9	126	2.3
7210 Haleakala	27	1237	3.7	209	1.2
7805 Metsahovi	5	62	21.7	34	15.1
7810 Zimmerwald	17	836	9.8	171	4.2
7833 Kootwijk	6	191	17.0	56	9.0
7834 Wettzell	30	1147	6.4	227	2.3
7835 Grasse	4	56	5.5	18	2.7
7837 Shanghai	3	18	11.0	11	11.0
7838 Simosato	24	842	3.9	138	1.2
7839 Graz	6	261	3.6	46	1.5
7840 Herstmonceux	31	1231	4.7	295	2.1
7886 Quincy/TLRS-1	3	248	6.8	32	2.4
7907 Arequipa	50	2146	14.2	375	5.7
7939 Matera	39	1818	13.8	419	6.3
Totals	450	19192	8.6	4194	1.5

TABLE 3. AUGUST 1984 LAGEOS FULL-RATE (FR) DATA AND THREE-MINUTE NORMAL POINTS (NP)

	Station	Passes	Number of FR Ranges	FR Precision (cm)	Number of NP Ranges	NP Precision (cm)	FR UTC
1181	Potsdam	17	382	17.6	86	8.3	BIH
7086	Ft. Davis	14	8210	6.9	138	0.8	USNO
7090	Yaragadee	14	74246	1.5	180	0.1	USNO
7105	Greenbelt	23	102386	2.5	239	0.1	USNO
7109	Quincy	54	382862	2.4	740	0.1	USNO
7110	Monument Peak	50	268043	2.4	553	0.1	USNO
7112	Platteville	13	1690	12.2	111	2.9	USNO
7121	Huahine	5	2781	8.2	40	0.9	USNO
7122	Mazatlan	14	34171	5.3	137	0.3	USNO
7210	Haleakala	25	64344	3.1	225	0.2	USNO
7805	Metsahovi	7	82	19.9	47	16.4	BIH
7810	Zimmerwald	13	4602	7.5	148	1.3	BIH
7833	Kootwijk	6	428	13.0	57	7.3	BIH
7834	Wettzell	30	19426	6.2	265	0.7	USNO
7835	Grasse	3	1832	7.1	27	0.7	BIH
7837	Shanghai	5	39	17.0	16	12.0	BIH
7838	Simosato	27	13656	9.1	166	1.0	USNO
7839	Graz	9	1616	3.6	59	0.7	TUG
7840	Herstmonceux	31	8001	4.5	299	0.8	BIH
7886	Quincy/TLRS-1	38	70596	6.4	434	0.5	USNO
7907	Arequipa	50	13578	14.4	550	2.8	USNO
7939	Matera	40	10378	13.7	495	2.8	USNO
Totals		488	1082882	4.0	5012	0.2	

TABLE 4. ESTIMATES OF STARLETTE QUICK-LOOK PRECISION DURING MERIT

		Precision Estimate (cm)
1148	Ondrejov	18.7
1181	Potsdam	19.1
1873	Simeiz	21.0
7090	Yaragadee	2.2
7105	Greenbelt	4.7
7109	Quincy	3.1
7110	Monument Peak	2.9
7112	Platteville	8.9
7121	Huahine	6.8
7122	Mazatlan	9.6
7210	Haleakala	3.6
7810	Zimmerwald	16.1
7833	Kootwijk	16.7
7834	Wettzell	7.5
7835	Grasse	4.2
7838	Simosato	7.6
7839	Graz	3.5
7840	Herstmonceux	5.3
7907	Arequipa	10.6
7935	Dodair	16.1
7939	Matera	9.1
7940	Dionysos	17.5

Edit criteria: 30 cm

Analysis of other stations is incomplete.

FIGURE 1

LAGEOS TRACKING FROM 8 MAY 1976 TO 31 SEPTEMBER 1984
PASSES IN 5 DAY BINS

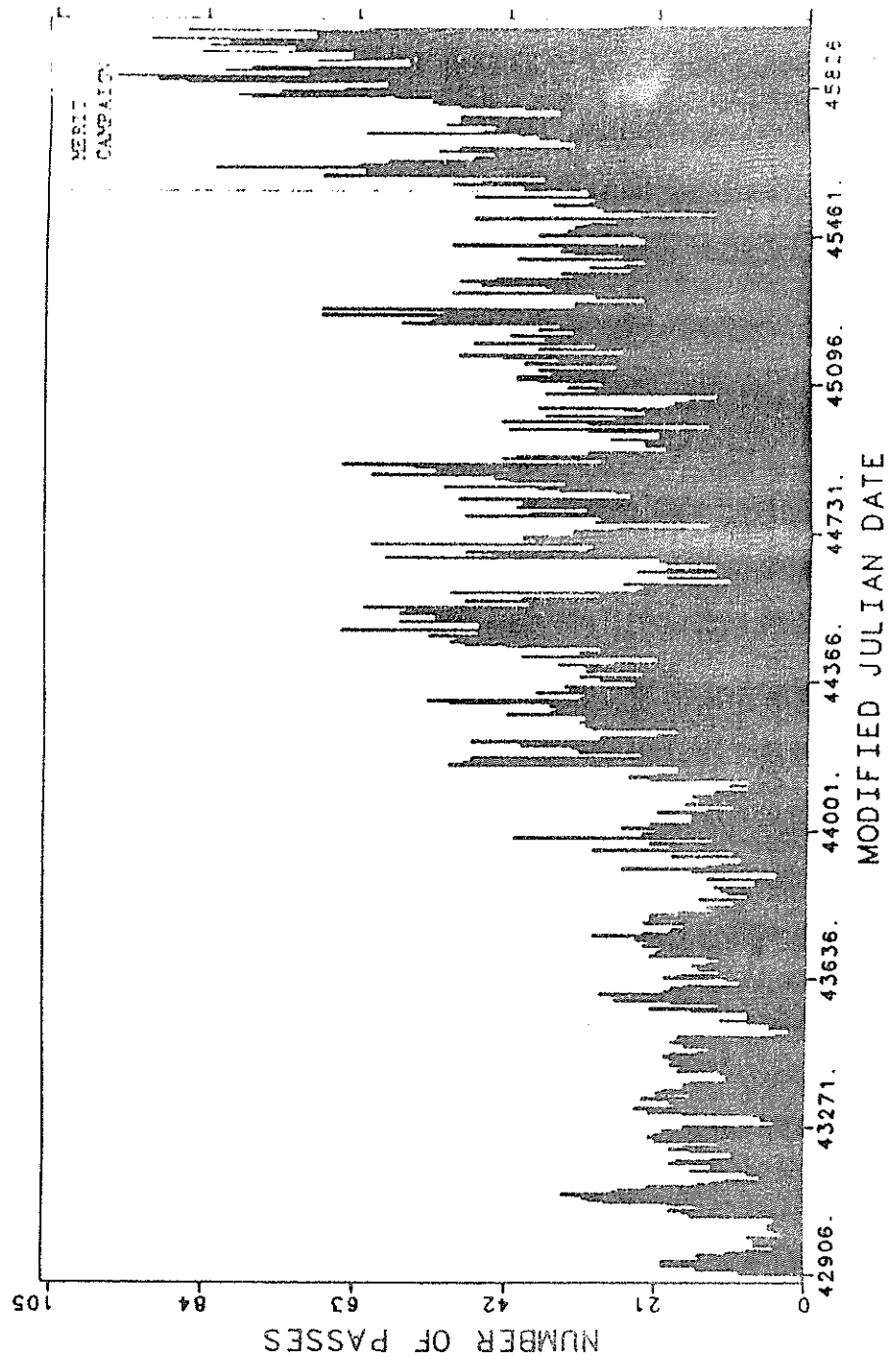

CURRENT DEVELOPMENTS IN EVENT TIMERS AT THE UNIVERSITY OF MARYLAND

C.A. Steggerda
Dept. of Physics and Astronomy
University of Maryland
College Park, Maryland 20742 USA

Telephone (301) 454 3405
Telex 908787

ABSTRACT

The Maryland dual slope Event Timer resolution has been improved to 50 ps. A dual frequency one stop Event Timer with resolution of 20 ps is under development.

The dual slope Event Timer originally developed in 1973 [1] has been updated and improved to have a 50 ps resolution. Specifically, the charging resistors affecting the dual slope sweep were changed so that the ratio of the slopes of the two sweeps is 250 to 1 instead of 125 to 1. This change causes the vernier to divide the basic 10 MHz clock rate into 2000 parts instead of 1000 parts. One of the MECL II integrated circuits was updated to its MECL 10K equivalent. The start amplifier has been replaced with a Tennelec model 455 Quad. constant fraction discriminator and LEMO connectors have been installed on all input ports for ease in maintenance and operation. The Event Timer can be run in the conventional single input mode which will allow detection of four events each about 6 nsec apart, or, with a small modification, the system can be made into four independent single event Event Timers.

A dual frequency Event Timer using the vernier principle of the Hewlett Packard 5370A[2] interpolator is currently under development. The Event Timer has a resolution of 20 ps and should be able to make two measurements 2 μs apart using one vernier. The Event Timer is connected to a microprocessor to form a time of day clock, range gate and Event Timer system. The micro processor puts the data in an IEEE format and interprets the IEEE format for the range gate. The Event Timer may be synchronized to either a 5 or 10 MHz standard or may operate alone with reduced accuracy.

A block diagram of the present form of the new Event Timer is shown in Figure 1. A 5 or 10 MHz external frequency standard is applied to one of the input ports of a phase detector while the 200 MHz signal generated by a voltage controlled crystal oscillator is divided by 40 or 20 and applied to the other input. The D.C. output of the phase detector controls the voltage controlled crystal oscillator which generates F_o = 200 MHz. This is one of the dual frequencies.

In the absence of an input pulse, a delay line oscillator, made by Hewlett Packard, generates a second frequency, F_1= 199.2217899 MHz, which will be referred to as F_1 or 199* MHz. The two frequencies F_o and F_1 are applied to the "D" and "clock" inputs of a "D type" flip flop which is used as a mixer. The output of the mixer is a square wave with a period of 1.285 μs and a frequency (F_o - F_1) of .778210 MHz. The beat frequency (F_o - F_1) is further synchronized to F_1 by the Sync. F.F., and applied to one of the inputs of a phase comparator while the second input of the comparator is supplied by (F_1 ÷ 256).

(1) 1973 A Precision Event Timer for Lunar Ranging, University of Maryland Department of Physics and Astronomy Tech Report 74-038.
(2) Manual for Hewlett Packard 5370A Universal Time Interval Counter.

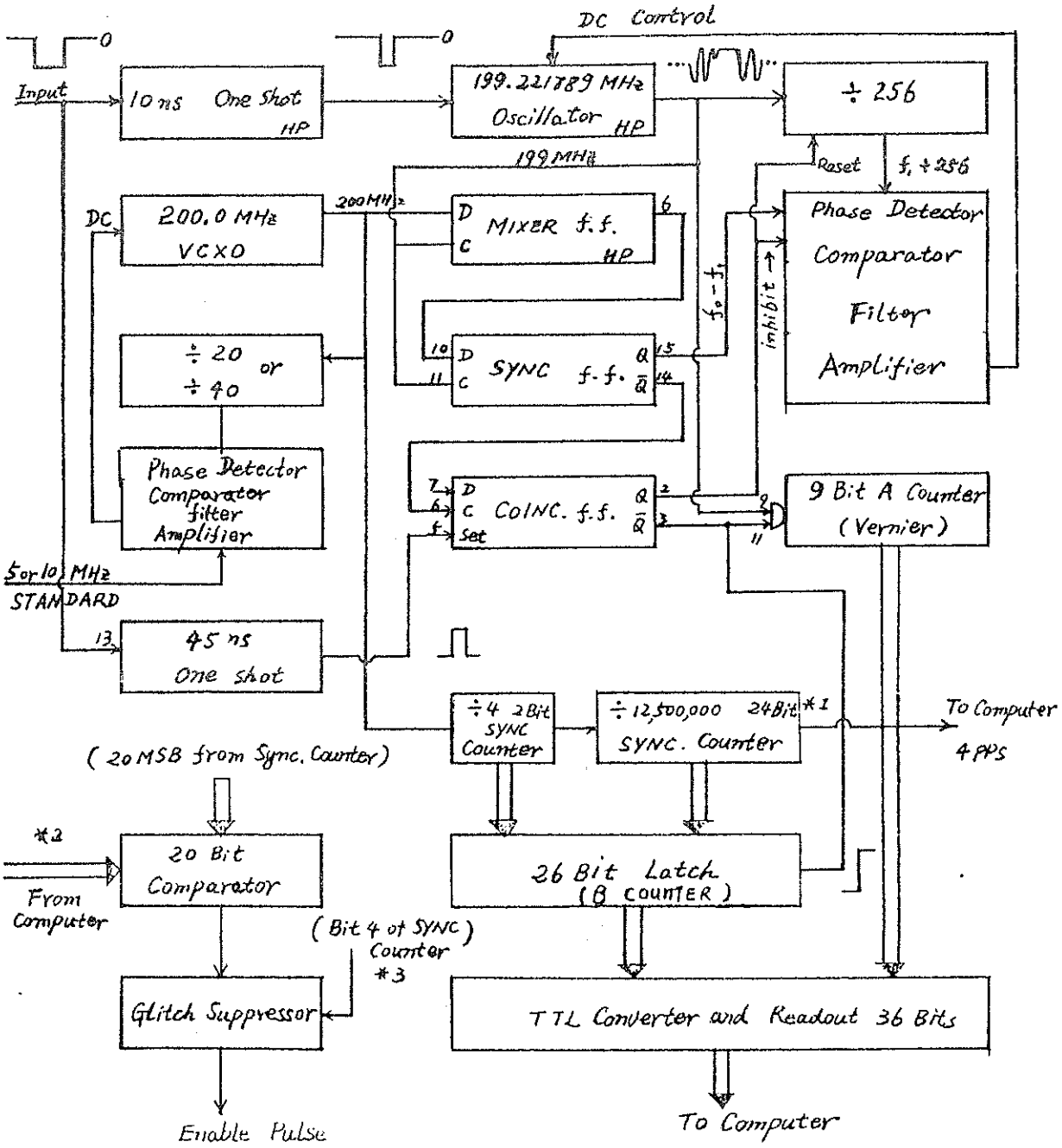

*1: THE 24 BIT COUNTER HAS $16,777,216_{(10)}$ STATES TO DIVIDE BY 12,500,000 THERE MUST BE 12,500,000 STATES SO
LAST COUNT = $16,777,215_{(10)} = 77,777,777_{(8)}$
FIRST COUNT = $4,277,216_{(10)} = 20,241,740_{(8)}$

*2: THE COMPUTER SENDS THE 20 MSB'S OF THE SYNC. COUNTER CODE $77,777,760_{(8)} \geq N \geq 20,241,740$

*3: BIT 4 (FROM LSB) RESOLUTION OF 320 ns

EVENT TIMER BLOCK DIAGRAM

figure 1

The comparator output is a D.C. voltage used to control the 199* MHz oscillator and to establish the equation:

$$(F_o - F_1) = F_1/256$$

which establishes the frequency F_1.

F_o is applied to the clock line of a 26 bit synchronous counter which consists of a two bit pre-scaler and a 24 bit synchronous counter which is adjusted to count exactly 12,500,000 states. The counter drive signals are adjusted so that in combination the two counters appear as one 26 bit synchronous counter with 50,000,000 states. The output of the synchronous counter is a pulse 4 times per second which is counted by the computer to form the time of day.

The rising edge, going from -.70 to 0 volts, of the input pulse, starts the Event Timer. In the test circuit the trailing edge of a negative going 30 ns pulse both edges of which are very precisely synchronized to F_o, activates the Event Timer. When a PMT is used, the input quiescent state will be -.70 volts and the leading edge of a positive going pulse is the starting event. This rising edge triggers a very precise 10 ns phase disconnect one shot.

The phase disconnect one shot stops the 199* MHz oscillator for about two cycles. When the oscillator restarts, hopefully, the frequency remains constant but the phase of the oscillation is synchronized to the input pulse rising edge. The rising edge of the input pulse also triggers a 45 ns anti-coincidence one shot which forces the coincidence F.F. to the set state. When the coincidence F.F. is set, the divide by 256 counter is held in the reset position, the phase detector is inhibited so that the D.C. control does not change, and a 9 bit "A counter" is enabled to count pulses from the 199* MHz oscillator occuring after the input pulse. After 45 ns, the set signal is removed and the coincidence F.F. is allowed to reset on the next synchronizer pulse which occurs when F_o and F_1 have the proper over-lap to cause the mixer to change state. When the co-incidence F.F. is reset, the divide by 256 counter is allowed to count from zero, the phase detector is reactivated, the "A counter" is stopped with the total number of counts proportional to the time from T, the time of the event, to the time of coincidence; and, a 26 bit latch or "B counter" stores the state of the synchronous counter when coincidence occurred.

Referring to Figure 2, at the end of the cycle of events, the "A counter" contains the number of 199* MHz (or 5.0195 ns) pulses from the event being timed to coincidence, the "B counter" contains the state of the 26 bit synchronous counter which is a measure of the number of 200 MHz (or 5.00 ns) pulses from the last 1/4 second to coincidence, and the phase locked loop is again closed with very little perturbations of F_1 due to the way that the divide by 256 counter is restarted at the time of coincidence.

THE EVENT TIMER HAS TWO OUTPUT REGISTERS, THE 9 BIT A REGISTER RECORDS THE NUMBER OF 199 * MHZ CYCLES FROM THE EVENT MEASURED TO THE TIME OF CO-INCIDENCE. THE 26 BIT B REGISTER RECORDS THE NUMBER OF 200 MHZ CYCLES FROM THE LAST 1/4 SECOND TIME MARK TO THE TIME OF CO-INCIDENCE.

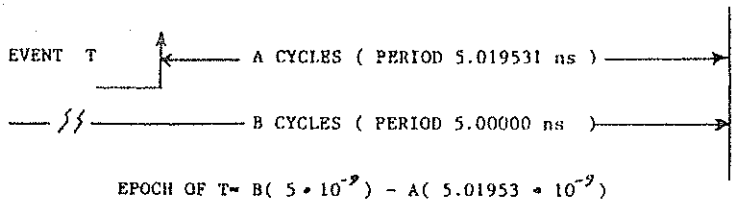

EPOCH OF T= B($5 * 10^{-9}$) - A($5.01953 * 10^{-9}$)

T= (B - A) * 10^{-9} - A($19.53 * 10^{-12}$)

DIAGRAM SHOWING HOW AN EPOCH MEASUREMET IS MADE

figure 2

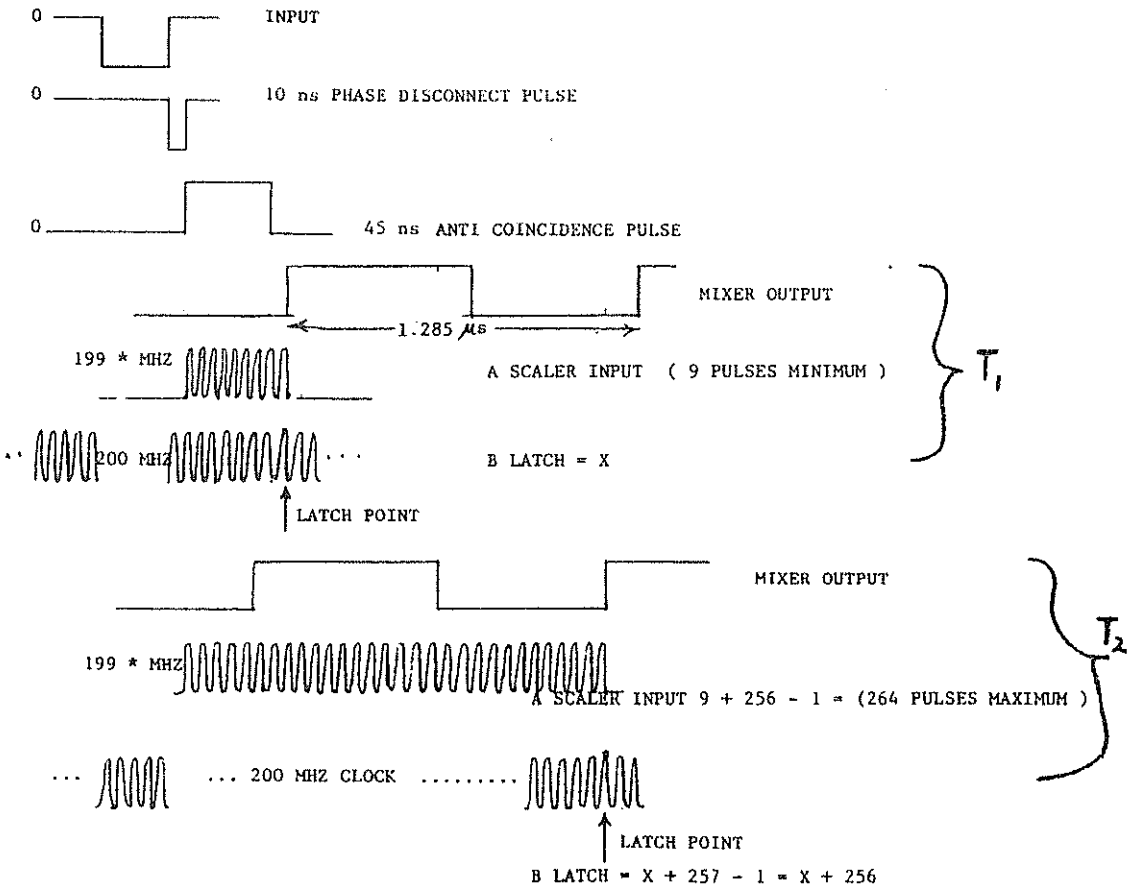

TIMING DIAGRAM SHOWING THE MEASUREMENT OF TWO PULSES T_1 AND T_2

(WHEN $T_2 = T_1 + .2500$ S. + 19.53 μS.)

figure 3

During measurements of the Event Timer, an input pulse was generated every 1/4 second and was synchronized very precisely with F_o. The phase of the input pulse with respect to F_o was adjusted with a "trombone" adjustable delay line. The adjustable delay line system made it possible to sweep over one entire 5 ns time period. Figure 3 shows what happens at the fold point when the A and B counters jump 256 and 257 counts respectively.

As the "trombone" delay line is adjusted, the point of coincidence as seen by the mixer output rising edge, comes progessively closer to the trailing edge of the anti-coincidence pulse. Further adjustment of the delay line moves the mixer rising edge inside the anti-coincidence pulse which blocks the coincidence F.F. from resetting. The result is that the "A counter" jumps 255 of the 5.01953 ns counts and the "B counter" jumps 256 of the 5.000 ns counts. Any deviation from this procedure results in an error when the epoch is calculated.

Figure 4 shows one of the prototype Event Timers and Figure 5 shows an interface card and an 8-bit microprocessor system used with the Event Timer. A great deal of effort has gone into making the fold-over point accurate. One of the problems that occurs is that when the 199* MHz oscillator is restarted during the measurement time, the oscillator is free running and its frequency will be slightly raised due to coupling to the 200 MHz. As soon as the phase locked loop is reclosed, F_1 returns to 199* MHz, but the fold-over point has too many counts. A further problem occurs if the "A counter" couples into F_1. This coupling appears to cause the odd states of the "A counter" to be favored over the even states. It is anticipated that these problems can be overcome however and that a 20 ps resolution Event Timer ca be built requiring no adjustments.

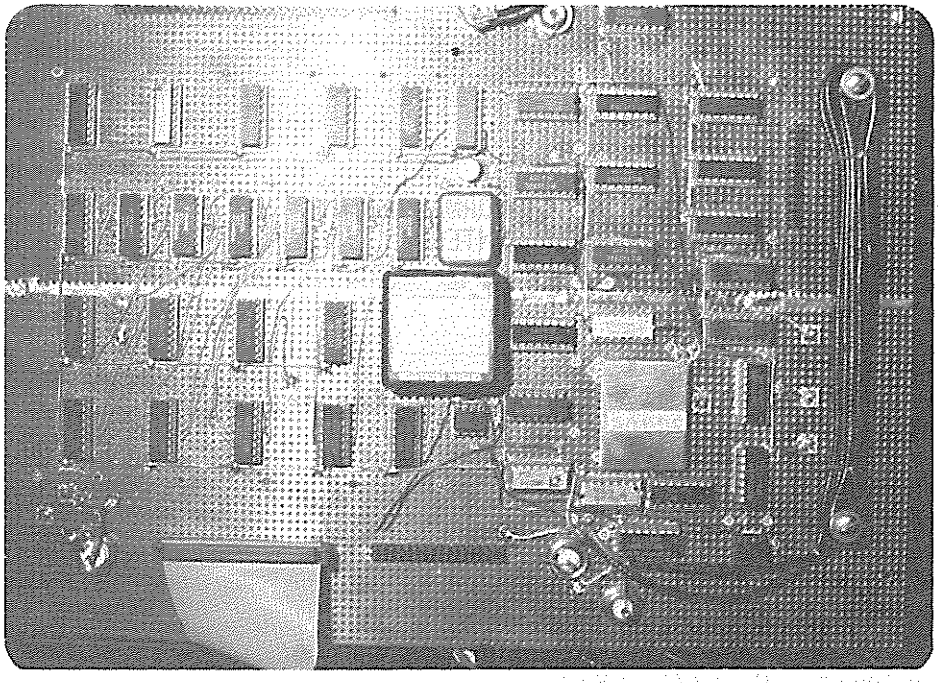

Figure 4 Prototype of Event Timer.

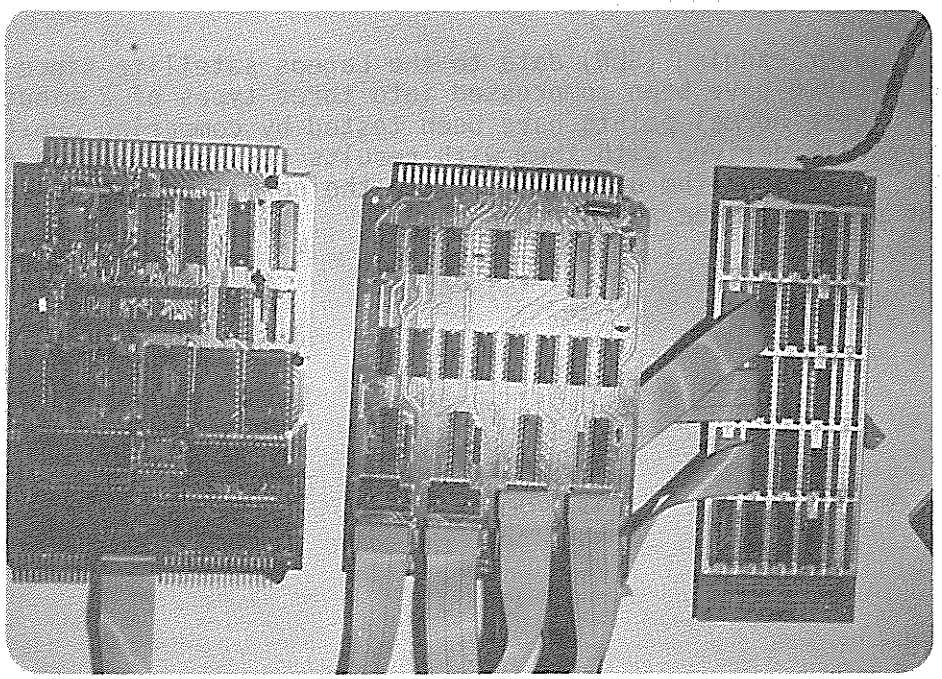

Figure 5 Interface and Microprocessor.

THE CONSTRUCTION AND TESTING OF NORMAL POINTS AT GODDARD SPACE FLIGHT CENTER

M.H. Torrence, S.M. Klosko
EG&G Washington Analytical Services Center, Inc.
Lanham, Maryland 20706, USA

Telephone (301) 731 2044
Telex 590613

D.C. Christodoulidis
Geodynamics Branch,
NASA Goddard Space Flight Center
Greenbelt, MD 20771 USA

Telephone (301) 344 7000
TWX 710 828 9716

ABSTRACT

Satellite laser ranging (SLR) data to the Lageos satellite since its launch in May of 1976 have been compressed into three types of 2 minutes normal points. These normal points have been tested by comparing orbital and geodetic results derived with them with results derived with the full rate SLR data. The alogorithm udes to generate the normal points is very similar to the proposal made at this workshop.

THE CONSTRUCTION AND TESTING OF NORMAL POINTS AT GODDARD SPACE FLIGHT CENTER

INTRODUCTION

At the National Aeronautics and Space Administration's Goddard Space Flight Center (GSFC), satellite laser ranging (SLR) data to the Lageos satellite has been compressed into normal points. Recently the SLR data has become so numerous, with current data rates of 1 to 5 points per second and almost thirty systems tracking worldwide, that some aggregation method has become necessary to avoid very costly analysis of the data. For a satellite such as Lageos, which is orbiting at nearly an earth's radius in altitude, utilization of data of this temporal density yields a redundancy of information which is approximately two orders of magnitude greater than that which is needed to fully monitor the perturbed motion of this satellite. While large data sets of independent observations reduce the influence of data noise on the calculated orbit, experience has shown that data noise is not a dominant error source for most applications of these data, and can be reduced through statistical methods which use the full data density to filter out the noise. The SLR data is compressed using temporal sampling based upon the presence of some minimum number of data points in the sampling interval. Other groups, Hauck and Lelgemann (1982) and Masters et al. (1983), have adopted methods to both thin the data while at the same time reducing noise in that data set. Masters et al. used successive differences in the second time derivative of the

range to edit the data and Chebyshev polynomial fits to short spans (150 sec) of the editted data to produce so called "laser normal points". This procedure accomplished three objectives: (1) outlying differences were used to edit anomalistic points, (2) the noise over these short spans was reduced by being averaged over the empirical function, and (3) filtered data, absent this noise, were produced. We have adopted similar procedures to accomplish these same objectives. Our approach was adopted to address not only the formation of normal points but also to assist with the assesment of the systematic stability of the laser systems, and their relative perfomance with respect to the other laser systems.

DEFINITIONS

Measurements inherently contain random error of observation. Ideally, the normal points associated with a given set of observations would be those same observations without the noise, i.e., the observations which would have been made if the process were noise free.

Consider laser ranging observations. The observed range at time t is

$$R_o(t) = R(t) + \varepsilon(t)$$

where $R(t)$ is the true range and

$\varepsilon(t)$ is the observational noise.

Mathematically, we can remove the error by averaging sufficient observations at time t so that the expected contribution of the random error to the average is insignificant. (for example, .1mm). In the real world there is only one measurement at each time t, and we rely on having observations at a rapid rate over a short period of time Δt. There must be sufficient observations during Δt so that the expected noise contribution is insignificant. The unmodelled change in the observation during this Δt must also have an insignificant contribution.

Because the noise removal must be performed over a non-zero time span, we have been required to introduce the concept of an observation model and a noise model.

We know that the true range at time t is given by

$$R(t) = f(O,S,A,t)$$

where f is a function of

- O the parameters defining the geocentric position of the instrument,

S the parameters describing the position of the satellite,

A the parameters describing the atmospheric effects.

That is to say, the range to the satellite at any time is the result of known modelable physical processes. These models are capable of predicting range at all times within a pass, not just at the times of the observations, to the same general level of accuracy: it is deterministic. (A pass is a set of tracking data which is acquired as the satellite goes from horizon to horizon.) There are errors in our modeling of the "true" range, $R_c(t)$. $R_c(t)$ is accurate to the decimeter level; our model of the evolution of the range in time is correct for the first seven or so significant figures. This error in $R_c(t)$ is the residual $\delta R(t)$ given by:

$$\delta R(t) = R(t) + \varepsilon(t) - R_c(t)$$

where $R(t)$ is the true noiseless range or the "normal" point range which is to be obtained.

Given a process, we would have normal points at each observation time. This is a very dense set, far more often than is required to demonstrate physical phenomena. Therefore, along with normal point creation (or noise removal) we also thin out the data. Typical practical solutions to this are decimation, interpolating the observation model to specified times, or just selecting the observation closest in time to the $\frac{\Delta t}{2}$ point - the bin midpoint.

Several considerations are necessary in order to construct normal points. First, we need to characterize the expected range as a function of time. Through knowledge of the spectral characteristics of the O, S, A above we can find a "sampling" interval (bin) which permits the reconstruction of all known "true" physical signals in the observed ranges from the thinned normal points.

Second, it is necessary to understand the behavior of δR within each bin. The spectra of δR and ε should be identical at short periods, i.e., the bin width, with some difference at longer periods due to unmodeled orbit errors. Harmonic analyses of the force model error perturbations on Lageos show no perturbation greater that a centimeter for periods of less than five minutes. Thus normal points formed from normally distributed data could safely be made at periods of less than 2.5 minutes. A numerical analysis of the order of the orbit integrator and the integration step size available for use in the computer program GEODYN (Putney, 1977) reveals that a good combination is a twelvth order integrator coupled with a 150 second step size. Both the error spectra of orbit

perturbations and the consideration of numerical accuracy has led us to choose two minutes for the bin to be used for forming normal points. On the basis of these analyses, we can state that the errors are modeled adequately by a low degree polynomial over a pass of residuals and may vary linearly within a properly selected bin width. This is a result of using an accurate R_c.

Therefore, we can state

$$R_N(t) \equiv R(t) = f(\delta R(t)) + R_c(t)$$

where $f(\delta R(t))$ is some functional representation over both the pass and the individual bin width which merely filters out, ε, the noise, and corrects our calculated range for the error in our models through the resulting signal in the range residuals.

We make three types of compressed range observations, or normal points, only one of which is a true normal point.

To do so, we follow these steps:

1. GEODYN, based on our best knowledge of the forces, etc. produces a set of residuals from 15 days worth of global range data

   $$\delta R(t) = R_o(t) - R_c(t)$$

2. A polynomial is fitted to the residuals to a pass of data

   $$\delta R(t) = g(t) + \xi(t)$$

   so each residual is then characterized in terms of signal and noise.

3. The remaining residuals are then:

   $$\delta r(t) = \delta R(t) - g(t)$$

4. δr is characterized by the mean residual in the bin

   $$\overline{\delta r}_b = \langle \delta r(t) \rangle + \langle \xi(t) \rangle$$

5. Form "poly-points" as:

   $$R_p(T) = g(T) + R_c(T)$$

   where T is time in the pass measured in two minute intervals from 0 hours UTC.

6. Form "bin corrected poly-points" as:

$$R_B(T) = g(T) + R_c(T) + \overline{\delta r}_b$$

where T is defined as in 5 above.

7. Form "true normal points" as:

$$R_N(t') = R_C(t') + g(t') + \overline{\delta r}_b$$

alternatively:

$$R_N(t') = R_o(t') - (\delta r(t) - \overline{\delta r}_b)$$

where t' is the time of an observation closest to the mean observation time within the bin.

See Figure 1 for a graphical representation of these data types.

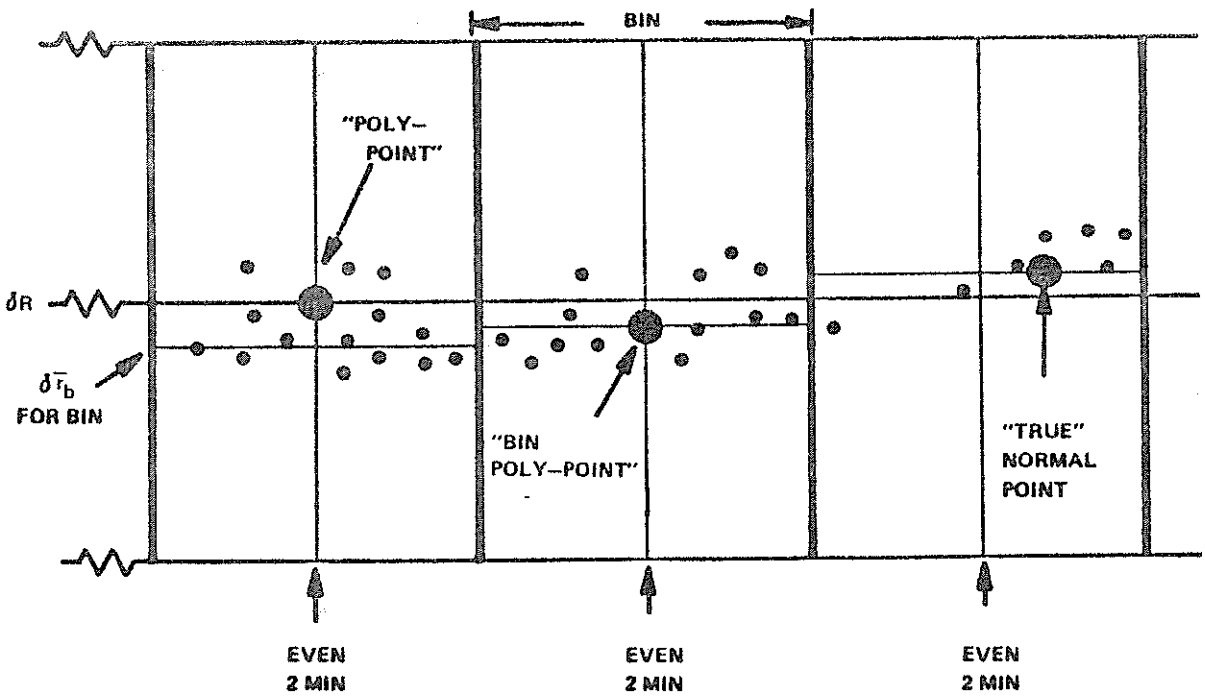

Figure 1.

Thus the "true" normal point noise at a specific point is estimated by the "signal" over the bin width. The noise error for a single point is then estimated and subtracted off the original range which is simply the true range (or normal point range) plus noise. Note also, our "true" normal point is at the time of a real observation. We have merely removed noise

from this observation to form a "normal point" at the mean observation time within each bin. This algorithm for "true" normal points conforms to the concept being put forth by this workshop.

VERIFICATION OF THE GSFC NORMAL POINT PROCEDURE

The Lageos range data is being taken to yield a data set to build an accurate model for the satellite's orbital motion to the accuracy of the data. The establishment of a reference frame defined by the orbit permits the accurate estimation of station positions and earth orientation parameters to help improve the understanding of the dynamics of the earth. In addition, improvements to and understanding of the force model is also accomplished. Thus, our testing philosophy was simple: do the normal points preserve the information content of the full rate data for calculating the Lageos orbit and for the recovery of station positions.

Three types of tests have been done to assess the performance of our normal points. For the first test, an orbit calculated with the full rate tracking data is fixed and station positions are adjusted. This is done with each of the three types of normal points and with the full rate data. The resulting sets of station positions are compared. The second test is the converse of the first; an orbit is converged with a fixed set of station positons. As before, this is done using the full rate data and each of the normal points data types individually. Then the four orbits are compared. The third test involves the convolution of the first two tests; the full rate data is used to converge an orbit and to solve for station positions, and the three types of normal points are used to converge the same orbit and solve for the same set of stations. The resulting orbits and station position are compared. The significance of these tests are evaluated by comparing the changes in the solved for quantities from the different data types with the formal errors.

TESTS FOR ORBIT RECOVERY: FIXING STATION POSITIONS

This test is to determine which, if any of the normal points can reproduce the orbit determined from the full rate data given the identical force model and station positions. Each normal point data type and the full rate data are used individually with the GEODYN program to solve for an epoch state vector for Lageos from the same time span of data. (For the purpose of this paper "state vector" refers to not only the position and velocity of Lageos but also includes the coefficients of along track acceleration and solar radiation pressure.) For this test each orbit determination is done with the same set of tracking stations which are not adjusted. When the true normal points were weighted at $1/\sqrt{n}$ m., where n is the number of fullrate points in the two minute bin, the state vector derived in the orbit determination reproduces the state vector determined from the full rate data when

that data is weighted at 1 m. If the true normal points were weighted at 1 m. the difference in the state vectors is significant, as is the case for uniformly weighted bin poly-points and poly-points. The true normal points, weighted at $1/\sqrt{n}$ m., reproduce the orbit recovered from the full rate data to a satisfactory level, but uniform weighting of the three normal point types is not equivalent to weighting the data by $1/\sqrt{n}$. Table 1 shows the difference of the x position and velocity component, along track acceleration, and coefficient of solar radiation from the corresponding quantity determined from the full rate data.

Table 1. Test of Orbit Adjustment: four fixed stations, 3 day arc

data type	weight (meters)	difference from apriori epoch full rate determination			
		ΔX (m)	$\Delta \dot{X}$ (m/s)	Accel $\times 10^{-11}$ m/sec^2	Cr
true normal point	$1/\sqrt{n}$	0.004	-0.004	0.001	0.0000
true normal point	1	0.793	-0.049	-0.049	0.0069
bin poly-point	1	0.847	-0.050	-0.044	0.0063
poly-point	1	0.793	-0.053	-0.041	0.0069

Tables 2 and 3 show the adjustments and their noise sigma of the epoch position and velocity from the same initial conditions for each of the normal point data types. These orbit determinations were done with four tracking stations and fifteen days of tracking data weighted at 0.10 m. Each of the four tracking stations had 0.10 m. quality full rate data and at least eight robust passes of data in the fifteen day span. The differences between adjustments from each normal point data type are small and not statistically significant. Thus orbits determined with any of the three normal point data types from robust, low noise data are equivalent.

Table 2. Test of Orbit Adjustment: four stations, 15 day arc, 0.1 m. weight

data type	adjustment from aprori position (meters)					
	ΔX	σX	ΔY	σY	ΔZ	σZ
true normal point	-0.430	0.024	-0.081	0.021	1.016	0.020
bin poly point	-0.439	0.026	-0.130	0.023	1.124	0.021
poly-point	-0.469	0.025	-0.104	0.023	1.121	0.021

Table 3. Test of Orbit Adjustment: four stations, 15 day arc, 0.1 m. weight

data type	adjustment from aprori velocity (meters/sec) ΔX	σX	ΔY	σY	ΔZ	σZ
true normal point	-0.019	0.042	-0.037	0.100	-0.014	0.042
bin poly-point	-0.023	0.042	-0.041	0.104	-0.015	0.042
poly-point	-0.022	0.041	-0.040	0.104	-0.015	0.042

TESTS FOR STATION RECOVERY: FIXING THE ORBIT

These tests are performed by comparing station positions determined from fifteen days of data in the presence of a fixed orbit. The data from each of the normal point types is weighted at 0.1 m. or $0.1/\sqrt{n}$ m. Table 4 shows the amount of adjustment and the noise sigmas of the adjustment in meters for the three data types.

Table 4. Test of Station Position Adjustment: 15 day arc, epoch state fixed

data type	weight (meters)	Earth Centered Component Adjustment (meters) ΔX	σX	ΔY	σY	ΔZ	σZ
true normal point	0.1	-0.137	0.021	-0.145	0.019	0.007	0.018
bin poly-point	0.1	-0.126	0.023	-0.142	0.020	0.002	0.019
poly-point	0.1	-0.121	0.023	-0.122	0.020	0.018	0.019
true normal point	$0.1/\sqrt{n}$	-0.114	0.017	-0.090	0.016	0.023	0.013
bin poly-point	$0.1/\sqrt{n}$	-0.104	0.017	-0.079	0.016	0.023	0.014

When the data are equally weighted, the differences between normal point types for each component adjustment of the station position are within the noise sigma of the adjustments. The RSS difference between the 0.1 m. weighted solutions are 0.012 m. for the true normal point minus the bin poly-point, and 0.036 m. for the true normal point minus the poly-point, and 0.026 m. for the bin poly-point minus the poly-point. These small numbers indicate that there is no significant difference between station positions determined from any of the uniformly weighted normal point types. This is also the case for a comparison between the uniformly weighted determination and the determination with the data weighted at $0.1/\sqrt{n}$ m. But, in this instance the RSS differences are larger than those above being 0.062 m for the true normal points and 0.070 for the bin poly-point.

TESTS FOR ORBIT AND STATION RECOVERY

This test is done by combining station position adjustment with state vector adjustment. For this test, a 15 day arc is determined with data from stations which had at least 10 passes of 3 cm precision data. Each type of normal points are weighted at 0.1 m in each of the least squares adjustment of the state vector and station position. Table 5 shows the resulting adjustment of a station position for each of the normal point types. There is no significant difference between these determinations.

Table 5. Station Position Adjustment: orbit adjusted, 5 day arc, 0.1 m. weights

data type	Earth Centered Component Adjustment (meters)					
	ΔX	σX	ΔY	σY	ΔZ	σZ
true normal points	-0.328	0.024	0.027	0.021	0.079	0.020
bin poly-points	-0.329	0.026	0.010	0.023	0.053	0.021
poly-points	-0.327	0.025	0.027	0.023	0.065	0.021

It is important to note, however, that station positions determined with sparse or noisy data weighted at 0.1 m. will show larger but still statistically insignificant differences between solutions done with the three types of data.

CONCLUSIONS

At GSFC, our analyses have shown that SLR data compression for the Lageos satellite is best done with two minute spans (bins) of full rate data. The algorthim we use to construct true normal points is virtually the same as recommended by this workshop, and we construct two other types of compressed data at the same time. From the analyses briefly reported above, we conclude that the true normal point constructed at GSFC can reproduce the results of the full rate data for state vector and station position determination when the true normal points are weighted at $1/\sqrt{n}$ m., where n is the number of points in the two minute bin. In addition, use of any of the normal point types, when equally weighted, to determine a state vector and/or station positions will produce results which differ insignificantly from each other.

ACKNOWLEDGMENTS

These investigations have profitted greatly from the participation of David Smith, Peter Dunn, Ron Kolenkiewicz, and Ron Williamson.

REFERENCES

Hauck, H., Lelgemann, D., "Die Bildung der Datenmittelwerte (normalpoints) aus Laserentfernungsmessungen. Arbeiten des Sonderforschungsbereiches 78 Satellitengeodäsie der TU München, Veröff.d.Bayer.Komm.f.d. Intern. Erdm., Astron.-Geod.Arb., Nr. 42, S.137-141 (1982).

Masters, E.G., Stoltz, A., Hirsch, 3., "On Filtering and Compressing Lageos Laser Range Data," Bull. Geod. 57, 121-130, 1983.

Putney, B.H., "General Theory for Dynamic Satellite Geodesy," National Geodetic Satellite Program, NASA SP365, 1977.

FIRST LEUT MEETING

ROYAL GREENWICH OBSERVATORY, 12 SEPTEMBER 1984

List of participants :

B. SERENE	ESA/Toulouse
S. LESCHIUTTA	Politecnico di Torino
J. DOW	ESA/ESOC
F. PALUTAN	TELESPAZIO
B. BERTOTTI	Uni. di Pavia
M. LISTER	Naval Research Laboratory
M. PAUNONEN	Finnish Geodetic Institute
G. VEIS	National Tech. Univ. of Athens
E. VERMAAT	Observatory Kootwijk
W. BEEK	Observatory Kootwijk
R. DASSING	Satellitenbeobachtungsstation Wettzel
R. HOPFL	Satellitenbeobachtungsstation Wettzel
JF. MANGIN	C.E.R.G.A.
F. PIERRON	S.L.R. G.R.G.S., C.E.R.G.A.
G. KIRCHNER	Lustbühel Observatory
D. KIRCHNER	Graz Tech. University
G. De JONG	Van Swinden lab. (VSL)
J. PILKINGTON	Royal Greenwich Observatory
J. GAIGNEBET	G.R.G.S., C.E.R.G.A.
C. ALLEY	University of Maryland
P. KLOCKLER	University of Berne
M. BOLOIX	Observatorio de Marina San Fernado

A G E N D A

1. Adoption of the Agenda.
2. LEUT Organisation.
3. Status of LASSO on board METEOSAT-P2.
4. Status of participating Laser Stations (including technical aspects).
5. Communication Network.
6. Calibration.
7. A. O. B.
8. Date and place of next meeting.

The meeting was held on 12 September 1984 at Herstmonceux Castle during the Fifth International Workshop on Laser Ranging Instrumentation.

As this LEUT meeting was the first to be held since the revival of LASSO, Dr. SERENE presented the goals :

- restart the organisation and work of the group;
- establish good relationships between the participants.

1. ADOPTION OF THE AGENDA

The agenda was amended to include a proposal of USNO to implement its bulletin in IRS DDS (Annex 1).

2. LEUT ORGANISATION

The LEUT Group was chaired by two Co-Chairmen :

- Dr. B. SERENE (representing the European Space Agency),
- Prof. S. LEISCHIUTTA, Politecnico di Torino (representing the Users).

Mr. GAIGNEBET acted as Session Secretary.

The minutes of the meeting will be typed and distributed by ESA.

3. STATUS OF LASSO ONBOARD METEOSAT-P2

The package designed for SIRIO-2 is going to be implemented on the METEOSAT-P2 satellite, after refurbishment. Like SIRIO-2, the satellite is spun but at 100 rpm. Its main mission implies a high stability of the spin rate and the synchronisation signal for image-taking must be very accurate.

Now the retro-reflectors and the detection unit are located side by side.

The nominal position of the satellite after launch is 0^{o} in longitude for a duration of about one year. It should be moved over the Atlantic Ocean as soon as a METEOSAT Operational satellite is in operation at the same site. This will allow the USA to participte in the programme.

ESA has to provide the group members with more precise specifications of the spacecraft, in particular its structure, frequency of the manoeuvres. A history of the manoeuvres of the existing meteorological satellites is thought to be very useful by the off-line members (Messrs. BERTOTTI, DOW, LESCHIUTTA).

4. STATUS OF THE STATIONS

Stations at Grasse (2), Kootwijk, San Fernando and Graz will participate as from commissioning.

The station of the University of Maryland, GSFC, will participate as soon as the position of the satellite permits.

The station of the Finnish Geodetic Institute is ready but its northern position limits the possibilities of ranging.

Stations at Wetzell (FRG), Dyonisos (GR), Matera, Zimmerwall (CH) and Cagliari (I) are willing to participate but are not certain to be ready in time.

The Herstmonceux station (UK) is neither not able to nor interested in participation.

Off-line members are interested by the ranging data and hope that the satellite will be kept without manoeuvres for long periods.

BIH will participate, in collaboration with CERGA, in pre-processing the data (Stations Synchronisations), the results being implemented on IRS/DDS as well as being included in the BIH Bulletin.

Participation of Intercosmos network stations :

Potsdam is still willing to participate. They are willing to switch to a YAG picosecond laser.

Mrs. TATEVIAN is interested in participating and would like more documentation.

The laser station representatives are requested to fill in the questionnaire (Annex 3) and to return it to ESA.

5. COMMUNICATION NETWORK

ESA is willing to keep the arrangement set up for SIRIO-2, i.e. use of the ESA network IRS/DDS. Many users feel that as they are already connected to MK III this could be the best means. The compatibility with the procedure defined for SIRIO-2 has to be confirmed by ESRIN. In any case, participating members hope that the network will operate very early to restart the knowledge and habits.

The Users ask ESA to study the possibility of taking charge of the network. This problem was opened by Dr. SERENE who reminded the participants that the budget is fixed and every over-cost will be taken off the exploitation time (predicted for 3 years).

The members ask ESA to provide cost figures for the use of IRS/DDS (Annex 2).

- implementation of USNO Bulletin on IRS/DDS :

  The stations have unanimously expressed their interest in this implementation.

6. CALIBRATION

Mr. GAIGNEBET has to provide cost figures for calibration round trips to all participating stations.

7. NEXT MEETING

TBD.

RESOLUTIONS ADOPTED AT THE FIFTH (1984) INTERNATIONAL WORKSHOP ON LASER RANGING INSTRUMENTATION

==========

RESOLUTION 1 : On the dedication of the proceedings

The participants in the fifth (1984) International Workshop on Laser Ranging Instrumentation consider that the proceedings of the Workshop should be dedicated to Frank Zeeman, late engineer at the Observatory for Satellite Geodesy at Kootwijk, Netherlands, who made major contributions to the development of the techniques of satellite laser ranging.

RESOLUTION 2 : On the need for the continuation of Loran-C emissions

The participants in the fifth (1984) International Workshop on Laser Ranging Instrumentation :

considering that the closure of the Mediterranean Loran-C chain is now foreseen for the year 1985 instead of 1992 as previously planned, that other clossures can be foreseen, and that the Loran-C signals constitute the main time synchronisation system for the laser stations operating in the northern hemisphere ;

and recognizing the needs of the Agency responsible for the Loran-C chains to terminate this service, and the adequacy of the interval until the year 1992 to introduce other synchronisation means for the laser ranging stations ;

urge the Agency responsible for the Loran-C system to review the proposed closure and to delay it at least until alternative means for time synchronisation are available to the laser ranging community.

RESOLUTION 3 : On the generation of normal points and the exchange of SLR data

The participants in the Fifth (1984) International Workshop on Laser Ranging Instrumentation recommend that :

1) The technique identified as Recommendation 84A for SLR normal-point generation and data exchange be adopted as an approved technique for the aggragation of SLR data ;

2) Details of the formats to accomodate normal points should be formulated by IAG SSG-2.81 and the final formats should be published in the proceedings of this workshop ; the formats should (a) provide for information that will cover the highest available quick-look normal-point accuracy, including time connections, (b) enable the identification of the normal-point generation technique, and (c) be suitable for the efficient exchange of SLR data ;

3) All stations or their agencies should make every effort to provide quick-look normal points in accordance with Recommendation 84A as soon as possible after the formats are finalized.

Recommendation 84A : On SLR normal-point generation and data exchange

The procedures for engineering anlysis and data screening that take place before quick-look data are transmitted should include a data compression step to provide high-quality quick-look data for scientific applications and to provide for the further avaluation of the data by the individual station or operating agency. The aggregation of raw data into a satellite-dependent fixed-time interval by an appropriate technique will produce a "normal-point range" and associated statistical properties. The resulting normal points should be transmitted as quick-look observations and should include the transmission of the associated statistics as well as information to enable the reconstruction of a raw measurement within the fixed interval. The following general procedure is recommended :

(1) Use high-accuracy predictions to generate prediction-residuals PR. (PR = Observation - prediction : include best available estimate for a time-bias and possible UT1-correction ; predicted range must include refraction).

(2) Use a suitable range (and time) window to remove large outliers.

(3) Solve for a set of parameters (orbital parameters are preferable) to remove the systematic trends of the prediction residuals, not introducing spurious high-frequency signals into the trend-function f(p).

(4) Compute fit-residuals FR = PR - f(p), and identify remaining gross errors using a 3 criterion.

(5) Iterate the two previous steps until no more can be identified ; previously rejected observations should always be reconsidered.

(6) Subdivide the edited fit residuals into fixed intervals (bins) starting from 0^h UTC ; the bin size should be the following :

Lageos : 2 minutes
Starlette : 30 seconds
Others : to be decided

(7) Compute the mean value $\overline{FR}_1$ and the mean epoch of the fit residuals for each bin.

(8) Locate the particular observation O_i, with its fit residual FR_1, whose observation time t_i is nearest the mean epoch of the bin i.

(9) Compute the normal-point range NP_i for each bin i using

$$NP_i = O_i - (FR_i - \overline{FR}_i)$$

(10) Compute the root-mean-square deviation m_i of the fit residuals for bin i from their mean, using

$$m_i = \sqrt{((\sum (FR - \overline{FR_i}))/(n-i))} \quad \text{or} \quad m_i = \sigma \text{ if } n = 1.$$

(11) Report for each bin i :

t_i observation time

NP_i normal-point range

n_i number of observations in the bin i

$\overline{FR_i}$ mean value of FR in the bin i

m_i bin standard error of single observations

Also report : σ pass standard error of single observations

(12) Use the format that is specified by SSG 2.82 for normal-point quick-look data.

(13) Report both old and new messages for at least ten passes for each station at the beginning of the distribution of quick-look data as normal-point ranges.

(14) Continue to report screened full-rate data in the standard format to the established data centres.

RESOLUTION 4 : On the need for lunar laser ranging observations

The participants in the Fifth (1984) International Workshop on Laser Ranging Instrumentation :

recognising the need for lunar laser ranging (LLR) data for use in current comparative studies of earth rotation and references systems, the value of LLR data in many scientific investigations, and that for the first time three LLR stations (CERGA, McDonald 107 and MLRS) are simultaneously operational ;

commend these stations for their successful efforts ;

urge other stations (e.g. Orroral, MAUI, Wetzell and the Crimea) to become operational as soon as possible ;

and strongly encourage all stations to obtain high-quality LLR data during the second MERIT-COTES intensive campaign in 1985 (May 23-31 ; June 6-14, 21-24 ; July 6-14, 20-28).